

1 2 9 0



UNIVERSIDADE DE  
COIMBRA

Luís André Perpétuo Silva

**NMR ANALYSIS OF URINARY ACETAMINOPHEN-  
GLUCURONIDE ENRICHMENTS FROM  $^2\text{H}$  AND  $^{13}\text{C}$   
METABOLIC TRACERS IN MOUSE MODELS**

VOLUME 1

Dissertation in the context of the Master in Biochemistry under the supervision of Doctor John Griffith Jones and Professor Rui de Carvalho presented to the Department of Life Sciences of the Faculty of Sciences and Technology of the University of Coimbra

January of 2020



Faculty of Science and Technology of the University of Coimbra  
Department of Life Sciences

# NMR analysis of urinary acetaminophen- glucuronide enrichments from $^2\text{H}$ and $^{13}\text{C}$ metabolic tracers in mouse models

Luís André Perpétuo Silva

VOLUME 1

Dissertation in the context of the Master in Biochemistry under the supervision of Doctor John Griffith Jones and Professor Rui de Carvalho presented to the Department of Life Sciences of the Faculty of Sciences and Technology of the University of Coimbra

January of 2020



“And once the storm is over, you won’t remember how you made it through, how you managed to survive. You won’t even be sure, whether the storm is really over. But one thing is certain. When you come out of the storm, you won’t be the same person who walked in. That’s what this storm’s all about.”

Haruki Murakami



# Agradecimentos

Antes de mais eu gostava de agradecer a todo o grupo da Biocant por me receberem de braços abertos, e em especial ao Doutor John Griffith Jones e à Doutora Cristina Barosa que juntos me guiaram com sabedoria e paciência durante o último ano e meio. Com a experiência que me permitiram ter eu cresci imenso quer a nível pessoal, que a nível estudantil. Tem um mundo de significados e importância tão vasto que se torna difícil colocar em palavras, mas o facto de estar um passo mais próximo do meu sonho de me tornar investigador científico faz-me profundamente feliz.

Uma breve nota de agradecimento ao Doutor Rui de Albuquerque Carvalho, um dos melhores profissionais com quem contactei na minha curta experiência académica. Fico grato que os nossos caminhos se tenham cruzado e de me ter transmitido a paixão pelo mundo do metabolismo, e por me ter ensinado as bases que estou certo me irão ser úteis por muitos anos.

Quero também agradecer à minha família mais próxima. Não só pelo último ano em que estive aplicado na parte prática/laboratorial desta tese, mas por todos os 24 anos antes desse também. Esta é a minha oportunidade de mostrar o resultado de décadas de estudo e de agradecer por todo o apoio e suporte que me deram nesta jornada, desde que nasci até aqui.

Aos meus avós Alice e Carlos, Lurdes e António, aos meus pais Luís e Paula, à minha irmã e aos meus tios, o meu obrigado. Desde os momentos bons, aos momentos maus, quem eu sou é a soma de todas as experiências que tive até hoje, e se este é o resultado. No fundo, vendo os resultados, só tenho que agradecer pela família que tenho. Sei que não preciso de listar todas as maneiras em que cada um me ajudou porque cada um tem consciência do que fez. De ir comigo ao café comprar-me pasteis de nata para o lanche, a levar-me à escola/desporto todos os dias incessantemente, a dar-me almoço sempre que peço, sem fazer questões, e mesmo que não peça... Sempre disponíveis, sempre prestáveis. Como disse, nenhum de vós é perfeito, mas eu agradeço pela experiência que me deram e que fazem esta vida memorável. Uma nota especial para o meu falecido avô António, que infelizmente não está cá para ler este agradecimento, mas que era um Homem extraordinário e presto a minha palavra de respeito aqui.

Ao meu pai, um obrigado por sempre me apoiar nas minhas escolhas. Infelizmente a minha área de estudo é bastante específica, e os detalhes escapam à maioria das pessoas, no entanto o meu pai, sendo uma dessas pessoas, só lhe interessa que eu goste do que faça, e que isso me faça feliz.

Inês... Não sei se na altura em que estás a ler isto entendas na totalidade o que estou a querer dizer, mas tu tens mais importância para mim do que aquilo que imaginas. A uma primeira vista, pode parecer que por eu ser o irmão mais velho, sou eu quem te ajuda mais. Mas o simples facto de existires e de seres como és, dá-me força nos dias mais escuros. Dás-me um norte quando eu não só perdi o norte, mas quando já nem a bússola consigo encontrar.

Por fim, o meu maior obrigado de todos à minha mãe. Costuma ser cliché dizer que tem uma mãe tem tudo, ou coisas desse género que exageram a relação mãe-filho. Neste caso, nada poderia ser mais próximo da realidade.

Quando parece que todo o mundo está de costas viradas para mim, a minha mãe chega sempre a casa com a famosa frase “Olá meu lindo” e com um sorriso na cara. Não importa o quão cansada está, ou quantas dores tem. Quando ninguém é capaz de entender a situação em que estou ou aquilo que estou a dizer, ela entende. E quando não entende, aceita.

Durante alguns anos, toda a gente desistiu de mim. Nesses anos tive problemas de saúde, quer física quer mental. Nesses anos, eu passava 90% do meu tempo em casa porque não conseguia sequer imaginar sair. Nesses anos, não havia quem tivesse tempo de me ouvir e aos meus problemas. No entanto, sempre que penso nesse período de tempo, há uma pessoa que esteve sempre lá, paciente, carinhosa, dedicada, compreensiva, amiga, por ter a disponibilidade que tem, e por me fornecer o maior suporte que alguma vez podia pedir. Por muito que tente compreender, é algo que me passa completamente ao lado: o amor da minha mãe.

Desde companhia em noites difíceis, a idas ao médico, às refeições especiais, às noites mal dormidas e dias perdidos em preocupações comigo. És a minha mãe, e não poderia sequer imaginar alguém melhor para essa posição na minha vida.

Para terminar esta dedicatória especial a esta pessoa especial, eu gostava de deixar uma piada privada: “estás com um ar apetitoso”. Um beijinho, um abraço, e um obrigado infinito.

Esta tese é especialmente dedicada à minha mãe.

This project was funded by FCT-FEDER (02/SAICT/2017/028147) “The Role of Visceral Fructose Metabolism in the Development of Non-alcoholic Fatty Liver Disease”



This page is intentionally left blank



# Resumo

---

A sociedade contemporânea está repleta de casos de obesidade e diabetes tipo 2, com maior incidência em países desenvolvidos e a previsão para os próximos anos/décadas não é brilhante. Um dos principais componentes desta epidemia é o consumo de frutose que excede a base evolutiva em que os seres humanos estão inseridos, resultado no metabolismo desequilibrado de hidratos de carbono e lípidos.

Aqui propomo-nos a estudar o impacto da frutose no metabolismo hepático, utilizando ratinhos C57BL/6, que são suscetíveis à obesidade induzida pela dieta e diabetes tipo 2. A abordagem baseia-se na utilização da marcação de isótopos estáveis, nomeadamente  $^2\text{H}$  (que permite o estudo dos fluxos metabólicos de todos os precursores de nutrientes) e  $^{13}\text{C}$  (para estudar o destino específico dos carbonos da glucose e da frutose, com base no perfil de marcação de isotopómeros).

Este estudo foi realizado através da administração de paracetamol que se ligará ao precursor imediato do glicogénio (UDPG, glucose difosfato de uridina) via ligação glicosídica, originando um glucuronato (glucuronato-paracetamol). O glucuronato-paracetamol é excretado na urina como parte de um processo de destoxificação que ocorre no fígado, proporcionando um método de biópsia não invasiva que permite o estudo das vias metabólicas hepáticas.

Para a análise de RMN do glucuronato-paracetamol, o processo mais comumente utilizado é a derivatização para MAGL (Lactona Glucurónica Monoacetona). Como o foco deste estudo será em ratinhos e o protocolo de derivatização tem rendimentos reduzidos (rendimento aproximado de 30-50%), ele iria causar perdas significativas de material durante o processo de derivatização, invalidando a capacidade de progredir no estudo. Para resolver este problema, propomos também desenvolver e aperfeiçoar um processo de purificação com maior eficiência, nomeadamente utilizando colunas de SPE (rendimento aproximado de 80-92%).

## Palavras-Chave

Metabolismo Hepático, Frutose, Glucuronato-Paracetamol, Marcação de Isótopos, Colunas SPE

# Summary

---

Contemporary society abounds with cases of obesity and type 2 diabetes, with more incidence in developed countries, and the forecast for the upcoming years/decades is not bright. One of the key components of this epidemic is the consumption of fructose that exceeds the evolutionary basis in which humans exist, resulting in the unbalanced metabolism of carbohydrates and lipids.

Here we propose to study the impact that fructose has on hepatic metabolism, using C57BL/6 mice: a strain that is susceptible to diet-induced obesity and type 2 diabetes. The approach is based on the use of stable isotope labelling, namely  $^2\text{H}$  (that allows metabolic fluxes from all nutrient precursors to be studied) and  $^{13}\text{C}$  (in order to study the specific destiny of the carbons of glucose and fructose, based on the isotopomer labelling profile).

This study was realized by administrating acetaminophen (commonly known as paracetamol) that binds to the immediate precursor of glycogen (UDPG, uridine diphosphate glucose) via glycosidic bond, originating a glucuronide (AG, acetaminophen-glucuronide). AG is excreted in the urine as a part of a detoxification process that occurs in the liver, providing a non-invasive biopsy that allows the study of hepatic metabolic pathways.

For NMR analysis of the AG, the most commonly used process is the derivatization to MAGL (Monoacetone Glucuronic Lactone). Because the focus of this study will be on mice and the derivatization protocol is characterized by having low yields (approximate yield 30-50%), it would cause significant material losses during the derivatization process, invalidating the ability to progress in the study. To solve this problem we also propose developing and perfecting a purification process with a higher efficiency, namely using SPE-columns process (approximate yield 80-92%).

## Keywords

Hepatic metabolism, Fructose, Acetaminophen-Glucuronide, Isotope Labelling, SPE-columns

# Contents

---

Introduction.....	1
Fructose context in human history.....	1
Hepatic Glycogenesis .....	3
Use of Acetaminophen as a non-invasive chemical biopsy strategy.....	5
Derivatization of AG.....	7
DSC-18 SPE column purification .....	9
Assessment of hepatic glycogen metabolism using stable-isotope-tracers .....	10
Deuterated water .....	10
Carbon 13 Tracers .....	11
<sup>2</sup> H and <sup>13</sup> C NMR .....	13
Dissertation objectives .....	16
Methods.....	17
AG solubilisation in water.....	17
AG stability test.....	17
DSC-18 SPE columns .....	17
Urine spike with commercial AG.....	18
DSC-18 SPE column optimization .....	18
Human administration of acetaminophen.....	18
Mice .....	19
Acetaminophen-glucuronide hydrolysis .....	20
Glucuronic acid derivatization to MAGL.....	21
NMR experiments .....	22
Proton- <sup>1</sup> H.....	22
Deuterium- <sup>2</sup> H.....	22
Carbon-13- <sup>13</sup> C .....	23
Results and Discussion .....	25

DSC-18 SPE column protocol development.....	25
AG initial experiments and stability tests.....	25
DSC-18 SPE columns protocol development and optimization.....	27
<sup>2</sup> H and <sup>13</sup> C spectra acquisition: tests and optimization.....	35
Application of the developed protocol in mice under a High Sugar diet.....	38
<sup>13</sup> C NMR analysis on mice urine samples after [U- <sup>13</sup> C]fructose and [U- <sup>13</sup> C]glucose administration .....	41
<sup>2</sup> H NMR analysis of mice urinary samples with deuterium labelling from deuterated water.....	43
Conclusion.....	45
Future Perspectives.....	47
References.....	48

This page is intentionally left blank

# Acronyms

---

- A** Acetaminophen (free acetaminophen)  
**AG** Acetaminophen-Glucuronide  
**AS** Acetaminophen-Sulphate  
**ATP** Adenosine Triphosphate  
**BW%** Body Water percentage  
**DHAP** Dihydroxyacetone Phosphate  
**F-6-P** Fructose-6-Phosphate  
**FAD** Flavin Adenine Dinucleotide  
**G-1-P** Glucose-1-Phosphate  
**G-3-P** Glyceraldehyde-3-Phosphate  
**G-6-P** Glucose-6-Phosphate  
**GLUT** Glucose Transporter  
**GS** Glycogen Synthase  
**GSH** Glutathione  
**GSK-3** Glycogen Synthase Kinase 3  
**H1, H2, H3, H4, H5** Denomination for each position of the proton on the hexose ring (1-5)  
**HFCS** High Fructose Corn Syrup  
**IP** Intraperitoneal  
**IV** Intravenous  
**LD50** Median Lethal Dose  
**LiBH<sub>4</sub>** Lithium Borohydride  
**MAG** Monoacetone Glucose (1,2-O-Isopropylidene- $\alpha$ -D-glucofuranose)  
**MAGL** Monoacetone Glucuronic Lactone (1,2-O-Isopropylidene- $\alpha$ -D-glucofuranurono-6,3-lactone)  
**MAGLA** 5-O-acetyl Monoacetone Glucuronic Lactone (5-O-acetyl-1,2-O-isopropylidene- $\alpha$ -D-glucofuranurono-6,3-lactone)  
**MeOH** Methanol  
**MG** Menthol Glucuronide  
**NADP** Nicotinamide Adenine Dinucleotide Phosphate  
**NAFLD** Non-Alcoholic Fatty Liver Disease  
**Nm** Nanometres  
**NMR** Nuclear Magnetic Resonance  
**OAA** Oxaloacetate  
**pckA** Phosphoenolpyruvate Carboxykinase  
**pka** Acid dissociation constant  
**PEP** Phosphoenolpyruvate

**PKB** Protein Kinase B

**PPP** Pentose Phosphate Pathway

**SPE DSC-18** Solid Phase Extraction Discovery C-18

**TFA** Trifluoroacetic Acid

**UDPG** Uridine Diphosphate glucose

**[U-<sup>13</sup>C]** <sup>13</sup>C (carbon-13) uniformly labelled substrate

# List of Figures

---

Figure 1- Overall perspective of fructolysis pathway leading to glycogen and/or glucose synthesis, and respective enzymes .....	2
Figure 2- Direct (blue) and indirect (orange) pathways for glycogenesis with examples of two hexoses entering the pathway and being metabolized.....	4
Figure 3- Acetaminophen detoxification pathway that occurs in the liver (GSH- glutathione; NAPQI- <i>N</i> -acetyl- <i>p</i> -benzoquinone imine) .....	6
Figure 4- Derivatization of AG into MAG (monoacetone glucose), MAGL (monoacetone glucuronic lactone) and MAGLA (5- <i>O</i> -acetyl monoacetone glucuronic lactone) .....	7
Figure 5- AG <sup>13</sup> C isotopomers labelling resulting from the metabolism of [U- <sup>13</sup> C]glucose and [U- <sup>13</sup> C]fructose. Carbons correlation between the trioses and the hexose for the reaction involving the trioses DHAP and G-3-P and an aldolase, forming fructose-1-6-bisphosphate. ....	12
Figure 6- <sup>1</sup> H NMR from native urine sample spiked with commercial acetaminophen β-D-glucuronide, and the referred molecule with the glucuronide protons numbered with water peak saturation.....	14
Figure 7- Tecniplast™ Metabolic Cage for single mouse .....	20
Figure 8- <sup>13</sup> C NMR spectra of 10 μmol of commercial AG dissolved in 1-2 mL of distilled water with the numbered carbons of the glucuronide.....	25
Figure 9- <sup>1</sup> H NMR spectra of AG samples under different conditions: room temperature (native elution sample), 50 °C (elution sample put under 50 °C for 24 h previously to the <sup>1</sup> H NMR experiment) and 65 °C (elution sample put under 65 °C for 24 h previously to the <sup>1</sup> H NMR experiment). The spectra shown are not at the same scale .....	27
Figure 10- Graphical representation of the colorimetric results of the purification of AG using DSC-18 SPE column. Each sample was made in triplicate and is represented with different colours. Loading volumes (pre-acidic H <sub>2</sub> O), first washing phase (acidic H <sub>2</sub> O), elution with 10% methanol (fraction 1 to 5, averaging 1 mL per fraction) and final washing phase (100% methanol). The purple line represents the average value for each phase .....	29



Figure 11- <sup>1</sup> H NMR spectra from the results of using a SPE-column to purify AG from urine obtained after spike with commercial AG. H1 to H5 refers to the protons of the glycosidic moiety of the AG. First wash phase using acidic water (A), elution phase using 10% methanol in acidic water (A), elution phase using 10% methanol in acidic water (B), and a final wash phase with 100% methanol (C).....	30
Figure 12- Graph comparing the efficiency of using water with different pH (2.5 and 7 coloured with blue and orange, respectively) to wash the native human urine sample spiked with commercial AG in DSC-18 SPE columns .....	31
Figure 13- <sup>1</sup> H NMR spectra of the 10% MeOH elution of the 2-4 h human urine sample .....	33
Figure 14- <sup>1</sup> H NMR spectra of the column elution of urine sample with 4 mL of 10% methanol in acidic water. H1 to H5 refers to protons of the glycosidic moiety of AG .....	34
Figure 15- Deuterium spectra of a SPE column purified human urine sample after acetaminophen and deuterated water administration .....	35
Figure 16- <sup>1</sup> H NMR spectra of the 10% methanol in acidic water elution phase containing purified urinary AG at different conditions: fraction under 50 °C for 24 h before spectra acquisition (blue), same protocol but at 65 °C (green), adding TFA as the sample is loaded into the NMR tube (red).....	36
Figure 17- Comparison of the values for the average for mice under control and high sugar diet, separated according to the batch (A, B and C) with standard deviation error bars .....	40
Figure 18- <sup>13</sup> C NMR spectra of MAGL derivatized from urinary AG from mice under high sugar diet (55% fructose and 45% glucose) after administration of acetaminophen. Signals of carbons 1, 4 and 5 are showed, with identification of singlets (S), doublets (D) and quartets (Q). Mice chow was enriched with 20% [U- <sup>13</sup> C]fructose (HS2) and 20% [U- <sup>13</sup> C]glucose (HS1), correspondent to mouse A and B, respectively.....	41
Figure 19- <sup>2</sup> H spectrum of MAGL derivatized from mice urinary AG. Mice were administrated deuterated water (4% deuterium enrichment via IP injection) and acetaminophen resulting in deuterium labelling in AG. The spectrum showed is relative to a mouse under a high sugar diet (55% fructose and 45% glucose). Signals 1-5 are identified in the spectrum. ....	43

This page is intentionally left blank

# Introduction

---

## Fructose context in human history

Current studies show that cases of obesity and type 2 diabetes are increasing at an alarming rate all across the globe. A recent report estimates that in 2017 at least 451 million people worldwide have diabetes, and predicted that by the year 2045 it will rise to 693 million [1]. Although the previous study does not differentiate between type 1 and type 2 diabetes, another study estimates that in the United States approximately 90-95% of diagnosed cases of diabetes are type 2 and only 5-10% are type 1 diabetes [2]. This means that the estimated cases for diabetes for 2017 in the first article mentioned (Cho et al. 2018 [1]) are mostly cases of type 2 diabetes.

According to the American Diabetes Association, in 2015 approximately 9,4% of the North American population had diabetes, being the 7<sup>th</sup> leading cause of death in the United States [3].

One of the main factors for this epidemic is the increase of the consumption of refined carbohydrates, such as sucrose [4]. Some of the most common ways of refined sugar consumption is through soft drinks, sodas, sauces, canned fruit, cakes and candy. One type of refined sugar is high-fructose corn syrup (HFCS).

HFCS were first introduced in the food and beverages industries in the late 1960s as a carbohydrate sweetener. The increased culturing of corn led to a glut of corn-starch, whose conversion to HFCS presented a more lucrative alternative to traditional sweeteners such as sucrose. This in turn led to HFCS being increasingly used in US foods [5], [6].

HFCS is generated by hydrolysis of corn-starch to corn syrup that mostly contains glucose, followed by its isomerization to fructose. There are three categories of HFCS: HFCS-90 (10% glucose and 90% fructose), HFCS-42 (58% glucose and 42% fructose) and HFCS-55 (45% glucose and 55% fructose). HFCS represented approximately 40% of all added caloric sweeteners in the USA in 2004 [7].

Fructose is a sweet-tasting monosaccharide that is either naturally present, or is linked with glucose to form sucrose. Fructose is found in some vegetables, cereals, fruits and honey. These sources show variable percentages of fructose contents (0,7% in raw apricots; 7,6% in raw apples; 33,8% in dried raisins; among others) [8]. During most of human evolution, fructose was consumed infrequently and contributed a minor fraction of total caloric intake. From the second half of the 20<sup>th</sup> century onwards, fructose consumption (both as HFCS and sucrose) in Westernized societies had a sharp increase. High-fructose diets are now recognized to be implicated in causing insulin resistance, oxidative stress, decreased glucose tolerance and hypertension [9–11], as well as metabolic diseases such as type 2 diabetes and obesity.

Fructose metabolism leads to its conversion into fructose-1-phosphate by a fructokinase or, as an alternative route, into fructose-6-phosphate, although this specific hexokinase has low affinity for fructose and this route is considered minor. The fructose-1-phosphate obtained is converted by aldolase resulting in glyceraldehyde and DHAP (Figure 1) being then able to enter glycolysis or glycogenesis pathways. There is relatively low control of this pathway resulting in an overflow of carbons into the triose phosphate pool. Furthermore, fructose enhances the activation of pyruvate kinase, leading to an increased amount of pyruvate entering the Krebs cycle [12].

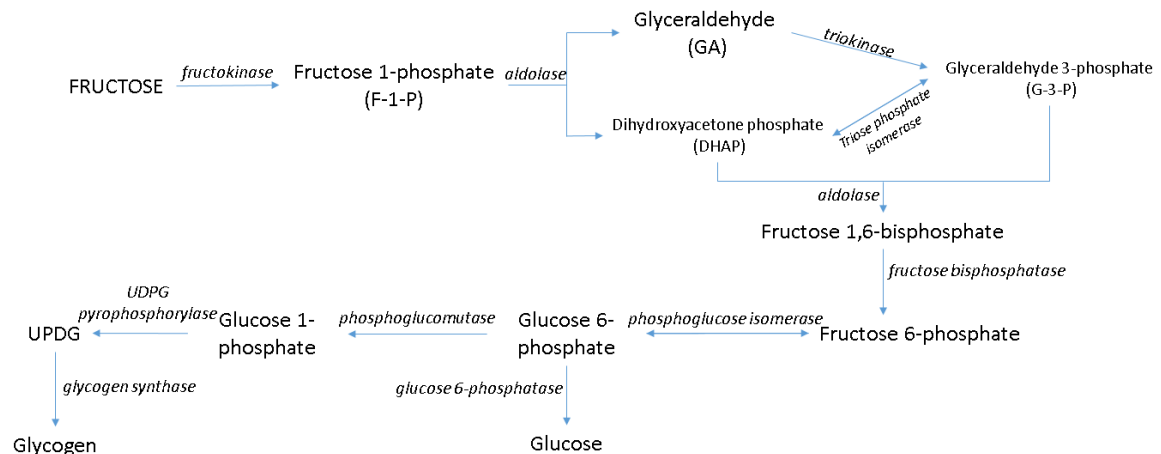


Figure 1- Overall perspective of fructolysis pathway leading to glycogen and/or glucose synthesis, and respective enzymes.

Fructose metabolism, in particular its conversion to glucose, is thought to be controlled by insulin [13]. Other studies showed that not only does fructose have a high impact on serum glucose levels, but it also modulates hormones such as the appetite-inducing hormone ghrelin and the appetite-inhibiting hormone leptin. Fructose and sucrose have been shown to activate the reward system in the hypothalamus [14].

In summary, the literature shows that the initial metabolism of fructose in humans, rats and mice is not strongly regulated; fructose has an impact in appetite-inducing/inhibiting hormones resulting in an overall increased caloric intake, and is an hedonic factor that stimulates further desire for consumption of foods with high sugar content. All these factors add up to make excessive fructose consumption a risk factor for NAFLD and type 2 diabetes.

## Hepatic Glycogenesis

In the fed state, the body stores glucose derived from dietary carbohydrate. Since glucose cannot be stored as it is, many glucose units are arranged to form a polymer, which is glycogen. This process is called glycogenesis, and the main storage organ of glycogen is the liver. Similarly to fructose, hepatic glycogen may also be involved in appetite control with changes in key regulators of food intake in the hypothalamus: animals with increased hepatic glycogen stores show less appetite [15].

Liver cells have insulin receptors in the cell membrane surface and, when bond to insulin, they become a dimer. The change in conformation leads to a cascade of kinase-mediated phosphorylations. This process affects protein kinase B (PKB). PKB is responsible for phosphorylating a monomeric G protein, stimulating the translocation of vesicles containing glucose transporters (GLUTs) into the cell membrane surface, allowing glucose to enter the cell through facilitated diffusion.

PKB is also responsible for phosphorylating glycogen synthase kinase (GSK-3), inhibiting it. The inhibition of GSK-3 activates the enzyme glycogen synthase (GS), promoting the synthesis of glycogen polymers. In fasting states however, blood insulin levels are lower and glucagon levels are higher. The liver will be in a state where GS is inhibited and glycogen phosphorylase (GP) is active, degrading glycogen into glucose [16].

This process has an impact in the whole body glucose levels: in a fasting state, insulin levels are high, glucose is prompted into entering cells in different tissues and in the liver the intracellular glucose is stored as glycogen. In a feeding state the insulin levels are low, and the liver is responsible for maintaining glycaemia levels within a certain range by starting to degrade the glycogen polymer and releasing glucose into the bloodstream.

There are two pathways for glycogenesis: the direct pathway (blue) and the indirect pathway (orange) (Figure 2). The direct pathway consists in a process where units of six carbons (hexoses) remain intact until they reach the glycogen polymer and merge with it. As showed in Figure 2, glucose (a hexose) is phosphorylated by glucokinase forming glucose-6-phosphate. The glucose-6-phosphate is converted it into glucose-1-phosphate via phosphoglucomutase, and then into UDPG by UDPG pyrophosphorylase. At this point, the glucose moiety is ready to be incorporated into glycogen via enzymatic reaction involving GS. This reaction combines the carbon 1 of the UDPG with the carbon 4 of the non-reducing end of a glycogen chain. Glucose in particular can also contribute to the indirect pathway by undergoing glycolysis and originating pyruvate (two pyruvates per glucose unit) that will then enter the indirect pathway.

The indirect pathway has some steps in common with the direct pathway, but does not maintain the hexose unit intact through all the process. The hexose breaks into two trioses at some point of the pathway (although it can begin with a triose), returning into a hexose further on.

Figure 2 shows fructose as an example of a hexose that is converted into trioses, namely glycerol-3-phosphate that has an equilibrium with dihydroxyacetone phosphate and, by the action of aldolase, turns into a hexose (fructose-1-6-biphosphate). This hexose loses one phosphate group through the enzymatic reaction with a phosphatase, and lastly an isomerase converts this fructose-6-phosphate (F-6-P) into a glucose-6-phosphate (G-6-P) that will follow the same reactions described for the direct pathway. Phosphoenolpyruvate (PEP) is also a precursor for the indirect pathway, having particular importance because of the phosphoenolpyruvate carboxykinase enzyme (pckA) that converts a Krebs cycle intermediate (oxaloacetate, OAA) to PEP. The labelling pattern of tracers that enter the Krebs cycle that are transmitted into glucose and glycogen via phosphoenolpyruvate provides a way to study fluxes through the Krebs cycle.

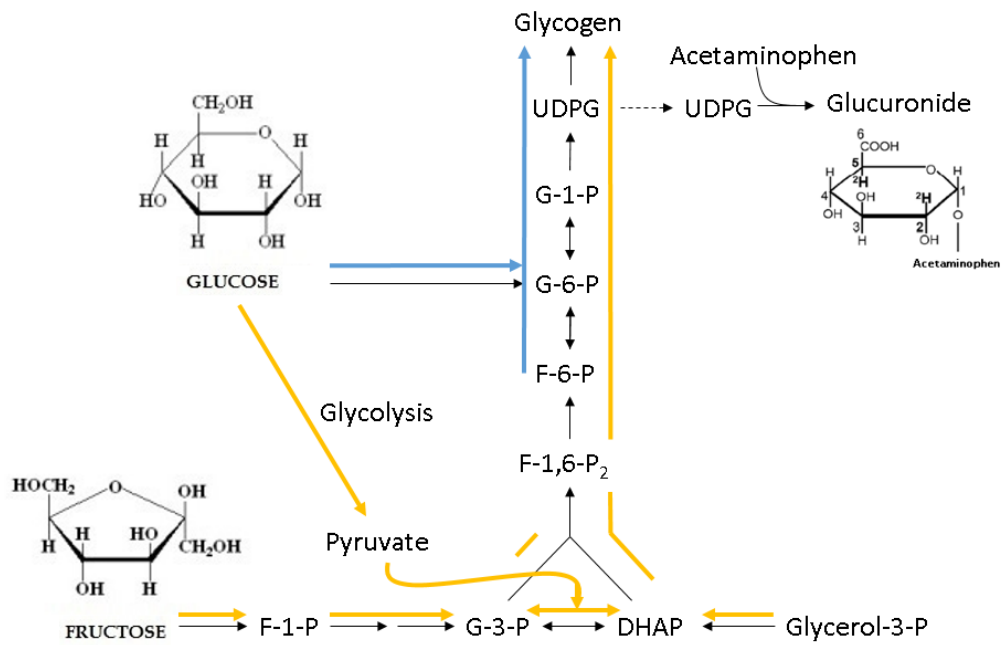


Figure 2- Direct (blue) and indirect (orange) pathways for glycogenesis with examples of two hexoses entering the pathway and being metabolized.

## Use of Acetaminophen as a non-invasive chemical biopsy strategy

There are examples of xenobiotics such as menthol [17] and acetaminophen [18], [23-24] (commonly known as paracetamol) being applied as a non-invasive way to perform a “chemical biopsy” in animals for metabolic studies. Not only this strategy improves data statistical significance in animal models, since the same individual can be used as experimental subject and its own control, but also this protocol can be used in humans. The fact that this can be translated into human studies boosts its magnitude and impact.

Acetaminophen binds to a glucose moiety of uridine diphosphate glucose (UDPG) via a glycosidic bond in the position 1 of the glucose ring, forming a glucuronide, as showed in Figure 2.

The glucuronide is then expelled in the urine as part of a detoxification process (for both menthol and acetaminophen) hence it is possible to collect the urine and analyse the glucuronide via NMR spectroscopy, avoiding the animal sacrifice. This protocol can be used in humans, providing a way to perform metabolic studies for diseases like diabetes type 2, obesity and even non-alcoholic fatty liver disease (NAFLD).

Menthol is metabolized to menthol-glucuronide (MG) and acetaminophen is also metabolized in a similar way to form acetaminophen-glucuronide (AG). Acetaminophen shows some disadvantages when compared to menthol: it has higher toxicity and is contraindicated for individuals with liver damage. Menthol administered via enteric capsules does not present any significant discomfort to humans [17] but in mouse models it has been reported to cause mouth lesions. Both acetaminophen and menthol have on rare occasions caused allergic reactions [28-29]. In terms of the glucuronide product, AG is more heat-stable than MG, which allows NMR spectra to be obtained at higher temperatures (seen in this thesis on “Methods” and “Discussion and Results”).

The detoxification pathway for acetaminophen occurs mostly in the liver (Figure 3). It is rapidly absorbed, with its rate of absorption limited only by the rate of gastric emptying [23]. Most of the acetaminophen administrated is immediately consumed by conjugation reactions including glucuronidation, but about 5-10% is converted into *N*-acetyl-*p*-benzoquinone imine via *N*-hydroxylation by the action of the P450 cytochrome [24]. This imine is conjugated with a glutathione (GSH) leading to harmless non-toxic metabolites, like cysteine and mercapturic acid conjugates. In case of an overdose of acetaminophen (human oral LD50 is 143 mg/kg, mouse oral and intraperitoneal (IP) LD50 are 338 mg/kg and 367 mg/kg, respectively [32-33]), this detoxification pathway is saturated and the imine can react with proteins and nucleic acids, which can cause liver failure, renal failure and, in extreme cases, death.

Therapeutic dosage of acetaminophen in human subjects ranges from 500 mg to 1000 mg per day, with a maximum dosage of 4000 mg per day. Intravenous (IV) administration of acetaminophen was approved by the US Food and Drug Administration in January 2011 at a dose of 15 mg/Kg every 6 h, not exceeding 60 mg/Kg/day [34-35] .

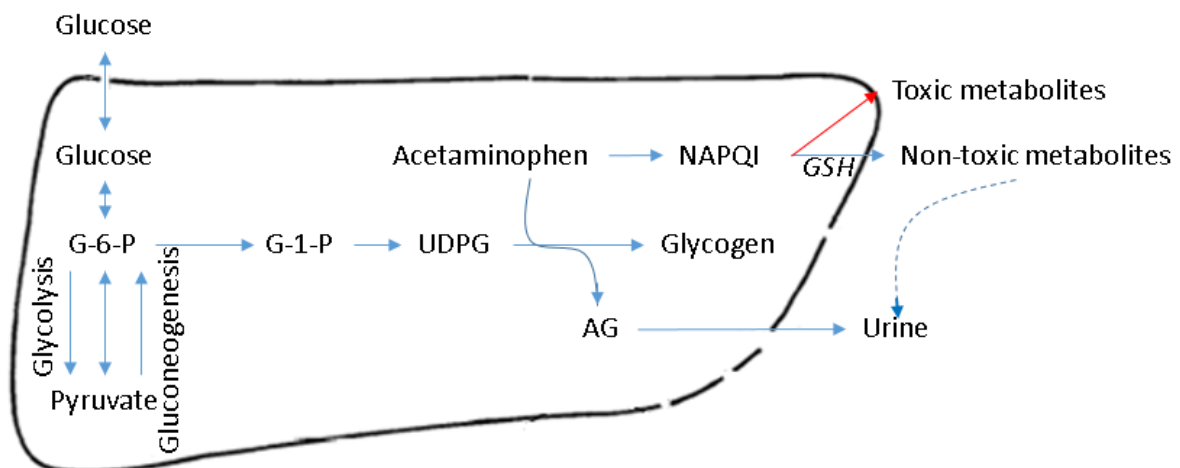


Figure 3- Acetaminophen detoxification pathway that occurs in the liver (GSH-glutathione; NAPQI- *N*-acetyl-*p*-benzoquinone imine).

Acetaminophen metabolism is similar in humans and mice, and results in three different metabolites: acetaminophen-glucuronide (AG), acetaminophen-sulphate (AS) and free acetaminophen (A). The relative percentages of each metabolite differ between individuals and species. AG usually presents itself as the major component with values around 72% in man and 55% in mice, AS is the second major component with approximately 27% in man and 10% in mice, and the free acetaminophen is usually presented in very small percentages, averaging 10% for both man and mice [36-37].

A more detailed approach to the use of acetaminophen as a non-invasive way to perform a metabolic study shows that, because acetaminophen conjugates with the precursor immediately before glycogen synthesis (UDPG), it allows the study of direct and indirect pathway activities and their contributions to glycogenesis.



## Derivatization of AG

To study the enrichment of UDPG (and by extension, newly synthesized glycogen) with  $^2\text{H}$  and  $^{13}\text{C}$  tracers by NMR, it has typically been derivatized in order to improve the dispersion of both  $^2\text{H}$  and  $^{13}\text{C}$  signals. Burgess et al. [19] developed a protocol with human subjects involving purification of AG from urine using DSC-18 SPE columns followed derivatization of AG to MAG.

In the NMR spectra of native AG, the fifth position signal of the glucuronide moiety lies very close to the water signal, and the signals corresponding to the positions 2 to 4 overlap severely with each other, making it impossible to quantify enrichments of these sites from the  $^2\text{H}$  NMR signals. While the position 1 signal is relatively well resolved, its enrichment from  $^2\text{H}_2\text{O}$  provides very limited information about glycogen synthesis fluxes. Thus, AG is typically derivatized into one of three molecules: monoacetone glucose (MAG, 1,2-O-Isopropylidene- $\alpha$ -D-glucofuranose), monoacetone glucuronic lactone (MAGL, 1,2-O-Isopropylidene- $\alpha$ -D-glucofuranurono-6,3-lactone) or 5-O-acetyl monoacetone glucuronic lactone (MAGLA, 5-O-acetyl-1,2-O-Isopropylidene- $\alpha$ -D-glucofuranurono-6,3-lactone), as seen in Figure 4.

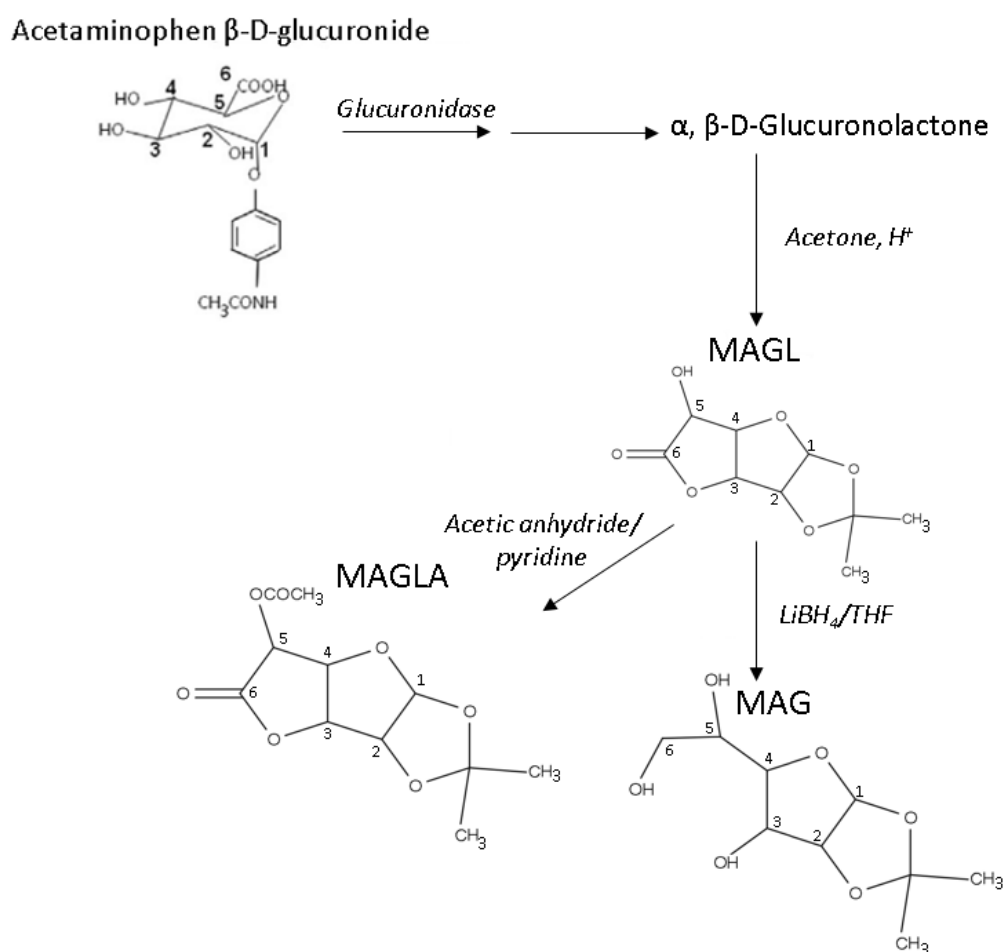


Figure 4- Derivatization of AG into MAG (monoacetone glucose), MAGL (monoacetone glucuronic lactone) and MAGLA (5-O-acetyl monoacetone glucuronic lactone).

Derivatization of AG to MAG is a tedious process and the yields are often unpredictable (40-80%) [20,35]. The MAG product has well resolved  $^2\text{H}$  and  $^{13}\text{C}$  NMR signals allowing complete analysis and quantification of all seven  $^2\text{H}$  and six  $^{13}\text{C}$ -enrichment sites of the hexose unit. One of the main uncertainties of this process is the reduction step using lithium borohydride ( $\text{LiBH}_4$ ) as the yield of this step is highly unpredictable.

An alternative to this problem is not reducing to MAG, but stopping the derivatization process in the molecule before: MAGL (Figure 4). While it eliminates the very troublesome reduction step, the MAGL deuterium NMR spectrum has a well-resolved position 5 signal, but the position 2 and 3 signals are overlapping. This means that it can be used if the interest of the study is determining the enrichment of position 5 relative to body water ( $\text{H5/body water}$ ), but is not suitable if the enrichment of position 2 relative to body water ( $\text{H2/body water}$ ) or  $\text{H5/H2}$  are required. With carbon-13 NMR spectra, all six hexose signals are fully resolved. Conversion of AG to MAGL is highly reproducible with yields ranging from 30% to 50% [20].

Acetylation of MAGL to MAGLA (Figure 4) is performed, using acetic anhydride and pyridine resolves the position 2 and 3 signals in the  $^2\text{H}$  NMR spectrum at 11.7 Tesla or higher [17]. The derivatization of AG to MAGLA shows an overall yield averaging 20-45% [20].

All molecules (MAG/MAGL/MAGLA) have some steps in common, as mentioned previously. This protocol is usually applied to urine samples obtained from humans, where at 2-4 hours after 1000 mg acetaminophen ingestion there is a range of urine production of 100-300 mL containing 300-900  $\mu\text{mol}$  of AG [17]. With these glucuronide quantities, the MAGL or MAGLA yields are such that deuterium NMR spectra with high signal-to-noise ratios are obtained providing a precise analysis of positional  $^2\text{H}$ -enrichments. Mice urine samples, on the other hand, have volumes averaging 1-2 mL, with AG yields of 10-20  $\mu\text{mol}$ , meaning that any loss during the derivatization process can have very significant impact on the signal-to-noise ratios of the spectra.

## DSC-18 SPE column purification

An alternative approach to the derivatization process mentioned previously is described by Burgess et al. [19]. The end goal is to simplify the purification and isolation process of AG. This method used perchloric acid to initially adjust the urine pH to approximately 4.5, and then maintain it while urease was added to remove urea, which can smother the DSC-18 SPE column surfaces. Urease is an enzyme that catalyzes the hydrolysis of urea into carbon dioxide and ammonia. As it produces ammonia, the pH of the sample increases and the enzyme becomes inactive. To maintain activity, the pH was continuously adjusted with perchloric acid. The sample was then loaded in a SPE column (after its preparation with acidic water), washed with acidic water, eluted with 10% methanol and a final wash with 100% methanol was also performed.

For the present study, this protocol was adapted from humans to mice. With the amounts of AG a factor of ten lower than in human samples, it is imperative that the protocol is optimized to minimize the loss of AG along the way. Another point of adapting the process is also to avoid the use of urease since maintaining the low pH required in such a small sample would be very troublesome. Since only the  $^2\text{H}$  signal in position 5 was required for this study (to quantify indirect pathway contribution by H5/body water enrichment [20]), the aim of this dissertation was to minimize the number of steps in the derivatization protocol that can provide this information. We thus chose to focus on AG to MAGL conversion since it yields a fully-resolved position 5  $^2\text{H}$  signal. The SPE column protocol was adapted to mice samples and perfected so that the final sample is pure enough to make the signal 5 quantification possible by deuterium NMR.

## Assessment of hepatic glycogen metabolism using stable-isotope-tracers

### Deuterated water

Deuterium is a stable isotope of hydrogen that has one neutron, giving an atomic mass of 2. Deuterium is found in nature at an abundance of 0.0015%. As a tracer, deuterium can be administered either in the form of deuterated substrates, for example [U- $^2\text{H}_7$ ]glucose, or as deuterated water, also known as heavy water ( $^2\text{H}_2\text{O}$ ).

The basis of  $^2\text{H}_2\text{O}$  as a metabolic tracer is that almost all cellular biosynthetic pathways directly or indirectly incorporate body water into their molecular structures. Thus, the  $^2\text{H}$  present in water will be incorporated into the bound hydrogens of any product that was synthesized by the cell, including carbohydrate, lipids, proteins and nucleotides.  $^2\text{H}_2\text{O}$  is rapidly distributed into all body water giving a constant level of body water  $^2\text{H}$ -enrichment in all tissues, organs and body fluids. In rats,  $^2\text{H}_2\text{O}$  is fully distributed into body water within 5 to 10 minutes following IP injection [31]. Deuterium distribution in humans takes somewhat longer: approximately 2 to 4 hours after oral ingestion of deuterated water [18-19].

For studies involving  $^2\text{H}_2\text{O}$ , the range of  $^2\text{H}$ -body water percentage (bw%) used for small animal models (3-5%) is approximately 10-fold higher compared to humans (0.3-0.5%) [19–21]. This is because bw% of 3-5% can be achieved by intraperitoneal injection of 99%  $^2\text{H}_2\text{O}$  in small animals while for humans it is administered by drinking with a limit of approximately 300-400 ml in one sitting.

Hepatic glycogen synthesis can be studied with  $^2\text{H}_2\text{O}$  since  $^2\text{H}$  from body water is incorporated into specific sites of newly synthesized glycogen hexose units, which reflect direct and indirect pathway activities.

The indirect pathway relative contribution to glycogenesis corresponds to the ratio between the deuterium enrichment found in the fifth position of AG and the total body water deuterium enrichment. Since the direct pathway has no  $^2\text{H}$  enrichment in the fifth position of AG, it does not contribute to the ratio mentioned above and this value is the result of subtracting the ratio of the indirect pathway to 1.

This fundament allows the differentiation of metabolic pathways: glucose metabolism in fed and fasted states, and the direct pathway from the indirect pathway. The direct pathway has water exchange steps that occur on the second position of the hexose ring, while the indirect pathway has water-exchanging steps for both second and fifth positions.

A brief note about the  $^2\text{H}$  labelling in the sixth position of MAG/MAGL/MAGLA obtained from hepatic glycogen purification and breakdown. The pathway that turns pyruvate into glyceraldehyde-3-phosphate contains a hydration step that converts phosphoenolpyruvate (PEP) into 2-phosphoglycerate (2-Phosphoglycerate). If deuterium is incorporated into the triose through this reaction, it will label the resulting hexose in the sixth position. The indirect pathway accounts for this contribution, since the resulting hexose is also labelled in the fifth position [35]. During the conversion of UDPG to UDP-glucuronic acid, the position 6 hydrogens are lost in the oxidation of the carbon 6 alcohol to carboxylic acid, hence AG does not retain  $^2\text{H}$ -enrichment in the sixth position.

Enrichment of the second position is due to the glucose-6-phosphatase isomerase reaction that interchanges glucose-6-phosphate with fructose-6-phosphate. During this reaction, there is a water hydrogen exchange step, labelling the glycogenic intermediate with  $^2\text{H}$ , specifically in the second position. This step is common for both direct and indirect pathways but the fifth position enrichment occurs only in the indirect pathway. The fifth position enrichment follows the same principal as the one mentioned for the second position enrichment, but is specific for the reaction involving a triose phosphate isomerase that exchanges dihydroxyacetone phosphate (DHAP) with glyceraldehyde-3-phosphate (G-3-P). DHAP and the G-3-P are converted into fructose-1,6-bisphosphate by the enzymatic reaction catalysed by aldolase. Thus, the second position enrichment in the triose phosphate becomes the fifth position enrichment in the hexose [35].

### Carbon 13 Tracers

Carbon tracers have also been used in studies of glycogen synthesis such as:  $[\text{U-}^{13}\text{C}_3]$ propionate,  $[\text{U-}^{13}\text{C}]$ glycerol,  $[\text{U-}^{13}\text{C}]$ galactose,  $[\text{U-}^{13}\text{C}]$ glucose and  $[1\text{-}^{13}\text{C}]$ glucose,[23-27,31-32].  $[\text{U-}^{13}\text{C}]$ glycerol was utilised to study gluconeogenic fluxes as well as  $[\text{U-}^{13}\text{C}]$ propionate: the latter was also applied to assess the hepatic Krebs cycle flux in human subjects, animal models and perfused livers.  $[\text{U-}^{13}\text{C}]$ galactose (in humans) and  $[\text{U-}^{13}\text{C}]$ glucose (in rats) were used to study the direct and indirect pathway contributions.  $[1\text{-}^{13}\text{C}]$ glucose was applied to study the hepatic glycogen kinetics in humans in periods of feeding and fasting.

Carbon-13 ( $^{13}\text{C}$ ) is a stable isotope, with six protons and seven neutrons (one more neutron than  $^{12}\text{C}$ ). Carbon-13 is found in nature at an abundance of 1.1%. Upon administration of uniformly-labelled  $[\text{U-}^{13}\text{C}]$ glucose, the glucose is taken up and metabolized. The  $^{13}\text{C}$ -containing metabolites can be detected by  $^{13}\text{C}$  nuclear magnetic resonance (NMR) spectroscopy.  $^{13}\text{C}$  labelling patterns in intracellular metabolites resulting from the metabolism a  $^{13}\text{C}$  labelled precursor, cellular uptake and secretion rates, and prior knowledge of the biochemical reaction network are combined to computationally estimate metabolic fluxes. In many cases, however, direct interpretation of  $^{13}\text{C}$  labelling patterns is sufficient to provide information on relative pathway activities, qualitative

changes in pathway contributions via alternative metabolic routes, and nutrient contributions to the production of different metabolites including glycogen. Although many carbon-13 tracers have been used in different studies, there have been few if any studies of hepatic glycogen enrichment from  $^{13}\text{C}$  enriched fructose.

By providing a way of measuring the contribution of a single specific substrate to glycogen synthesis, carbon tracers complement the information derived from  $^2\text{H}_2\text{O}$ .

The lack of previous studies using  $[\text{U}-^{13}\text{C}]$ fructose to analyse its contribution to hepatic glycogen synthesis means that predicting the outcome of using this tracer is not completely clear. Nevertheless, it is expected to have some similarities with  $[\text{U}-^{13}\text{C}]$ glucose labelling.

Direct pathway conversion of glucose to glycogen via G-6-P does not cleave the hexose carbon skeleton thus  $[\text{U}-^{13}\text{C}]$ glucose, and the relative contribution to glycogenesis is proportional to the amount of uniformly labelled tracer observed by  $^{13}\text{C}$  NMR analysis in glycogen (invasive biopsy) or in glucuronide (non-invasive biopsy).

The indirect pathway metabolism of glucose to glycogen involves its initial conversion to pyruvate via glycolysis, breaking the hexose into trioses.

The same principle as for the deuterium labelling also applies here: the probability that two labelled trioses bind to re-form an uniformly labelled hexose is insignificant.

Figure 5 shows the different glucuronide labelling patterns that result from the administration of  $[\text{U}-^{13}\text{C}]$ glucose and  $[\text{U}-^{13}\text{C}]$ fructose.

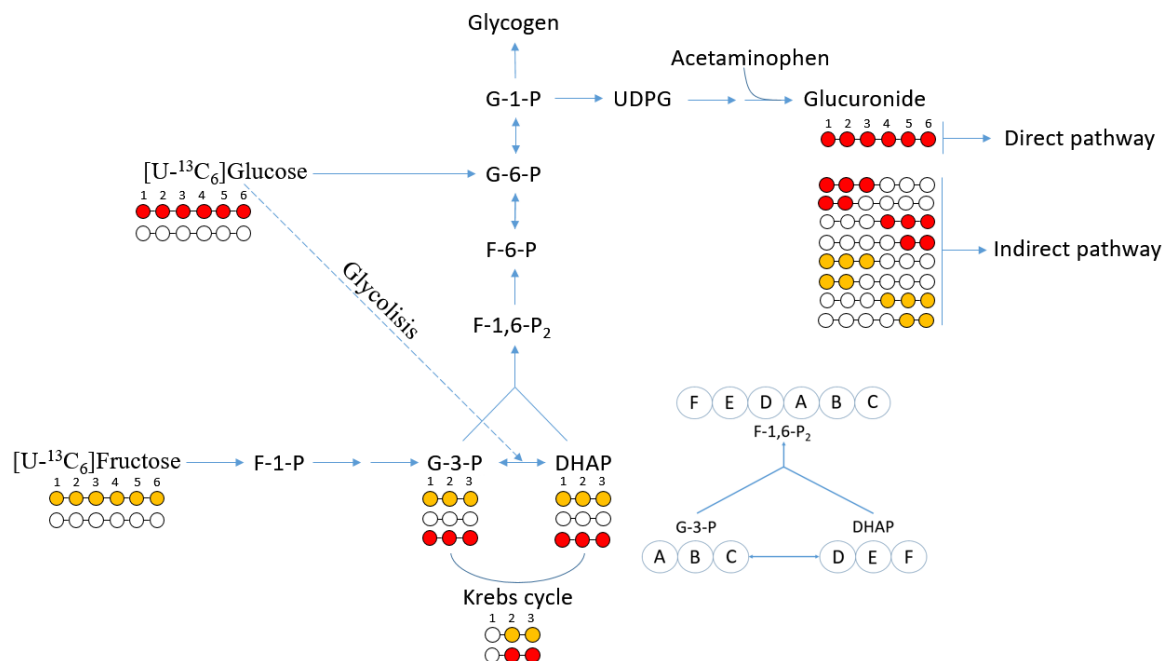


Figure 5- AG  $^{13}\text{C}$  isotopomers labelling resulting from the metabolism of  $[\text{U}-^{13}\text{C}]$ glucose and  $[\text{U}-^{13}\text{C}]$ fructose. Carbons correlation between the trioses and the hexose for the reaction involving the trioses DHAP and G-3-P and an aldolase, forming fructose-1-6-bisphosphate.

[U-<sup>13</sup>C]<sub>6</sub>glucose can be converted to glycogen by the direct pathway, with this route the hexose skeleton remains intact.

[U-<sup>13</sup>C]fructose is metabolized via the indirect pathway, where the hexose ring is broken, resulting in two trioses: DHAP and G-3-P. The trioses are merged together into a hexose in a specific order: DHAP carbons 1,2 and 3 correspond to carbons 3, 2 and 1 of the hexose (respectively), while G-3-P carbons 1, 2 and 3 correspond to carbons 4, 5 and 6 respectively (as showed in Figure 5).

The labelling difference between [1,2-<sup>13</sup>C<sub>3</sub>]AG and [5,6-<sup>13</sup>C<sub>3</sub>]AG is due to the activity of the pentose phosphate pathway (PPP). This was shown for individuals administered with [U-<sup>13</sup>C]glycerol [38], which is metabolized in a similar way to [U-<sup>13</sup>C]fructose.

## <sup>2</sup>H and <sup>13</sup>C NMR

Although carbon-13 NMR is far less sensitive than either <sup>13</sup>C-detection by mass spectrometry or <sup>14</sup>C radioisotope detection, it is widely used in metabolic studies because it is possible to precisely assign and quantify complex <sup>13</sup>C-labeling patterns in a variety of metabolites. <sup>13</sup>C NMR analysis can utilize on both invasive and non-invasive methods of metabolite extraction from tissues as described previously. This approach has been used to quantify metabolic fluxes through the hepatic Krebs cycle, gluconeogenesis and glycogenolysis [31, 39-40].

Analysis of metabolite <sup>2</sup>H-enrichment by deuterium NMR is relatively more recent than the <sup>13</sup>C NMR. <sup>2</sup>H has a low natural abundance but since it has a very short relaxation time, it is possible rapidly pulse the nucleus without saturation and acquire quantitative <sup>2</sup>H signals in a relatively short time period. This technique has been used to study the incorporation of <sup>2</sup>H from <sup>2</sup>H<sub>2</sub>O into a range of products including glycogen, lipids and proteins [20, 41-42], among other uses such as tumoral metabolic studies and hepatic glycogen kinetics in fasting and feeding states [33, 43-44].

<sup>1</sup>H and <sup>2</sup>H NMR signals of a given metabolite position are isochronous, that is, they have the same chemical shift values. Because of its quadrupolar relaxation, the <sup>2</sup>H NMR signals are inherently broader than those of <sup>1</sup>H. Moreover, the gyromagnetic ratio of <sup>2</sup>H is only about 1/7<sup>th</sup> that of <sup>1</sup>H hence the <sup>2</sup>H NMR signals are much more crowded together compared to those of <sup>1</sup>H. Because of this, it is imperative that the <sup>2</sup>H peak of interest is resolved from all other <sup>2</sup>H signals. Because of the isochronous nature of <sup>2</sup>H and <sup>1</sup>H signals, the <sup>2</sup>H signal resolution of a given sample can be in part predicted by inspection of the <sup>1</sup>H NMR spectrum. The <sup>1</sup>H NMR spectrum also provides information on the sample purity and can be used to verify that the observed <sup>2</sup>H signal is originating from the correct position of the correct molecule.

In this case, for the <sup>2</sup>H NMR experiment to be successful, the AG fifth signal needs to be resolved from all other peaks in the <sup>2</sup>H NMR spectrum. The signal closest to it is the water peak, and the

resolution can be improved by increasing the NMR acquisition temperature or changing solvents and modifying the chemical environment (all of which move the position of the water signal but leave the AG signal relatively unchanged). Figure 6 shows a spectrum from commercial AG that was added to an urine sample without AG. At 7.14-7.37 ppm there is a double-doublet from the AG aromatic ring, specifically from the acetaminophen moiety, between 3.6 and 5.1 ppm there are the signals from the hexose ring of AG. The signal 1 (H1) is a doublet that appears at 5.1 and 5.0 ppm, the signal 5 (H5) is a doublet at 3.89 and 3.90 ppm, and the remaining signals (H2-H4) are overlapping at around 3.6 ppm, and it is not possible to study or quantify any of the three signals. The methyl group peak from the acetaminophen moiety (singlet) appears at 2.16 ppm is used to quantify the amount of AG present on the sample. The quantification is made by weighing the sample that is put in the NMR tube and the NMR pyrazine standard (that was not used in the experiment showed in the Figure 6). Measuring the peak intensity and normalizing with the respective weight the quantification is then made.

The spectrum showed in Figure 6 has the water peak saturated (4.8 ppm), but this is not always the case. When the water peak is overlapping or very close to a signal, it cannot be saturated since it would also eradicate the signal. It is important to note that the ppm at which the signals appear may change upon the chemical environment, meaning that urine samples after acetaminophen administration and water samples with commercial acetaminophen  $\beta$ -D-glucuronide may present  $^1\text{H}$ ,  $^2\text{H}$  and  $^{13}\text{C}$  NMR peaks at different ppm.

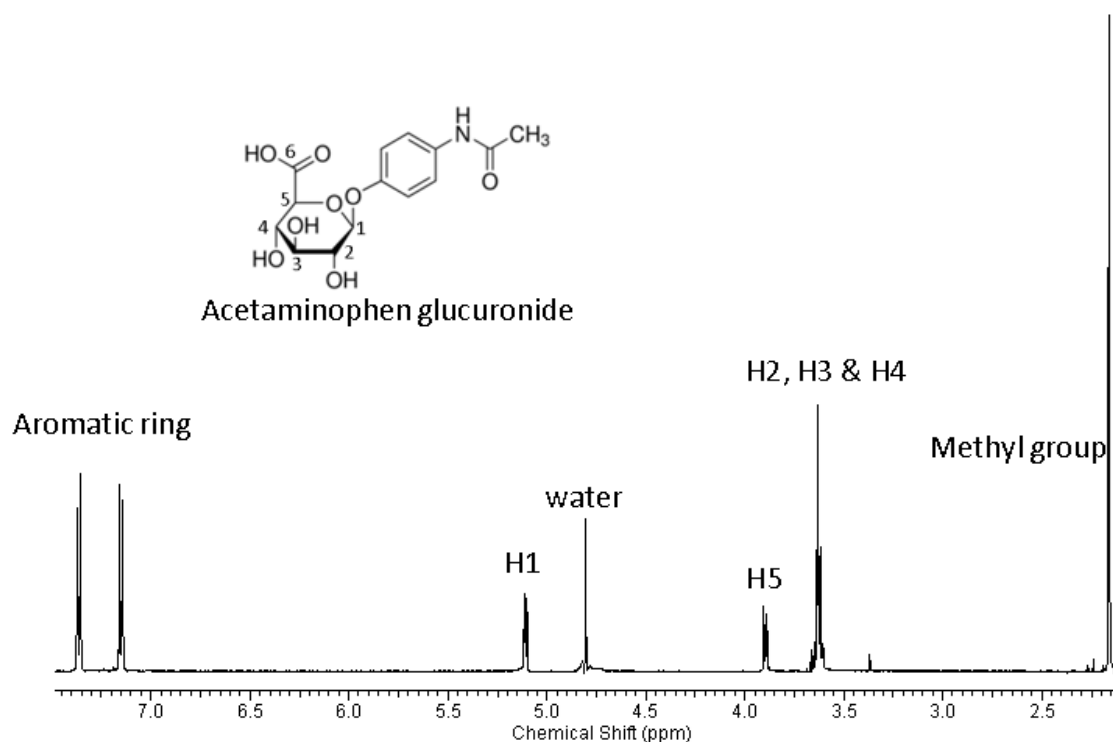


Figure 6-  $^1\text{H}$  NMR from native urine sample spiked with commercial acetaminophen  $\beta$ -D-glucuronide, and the referred molecule with the glucuronide protons numbered with water peak saturation.



There is also interest in studying the isotope labelling resulting from  $^{13}\text{C}$  labelled tracer administration, in this case uniformly labelled glucose and fructose ( $[\text{U-}^{13}\text{C}]\text{glucose}$  and  $[\text{U-}^{13}\text{C}]\text{fructose}$ ).

As explained before, glucose can contribute to the direct pathway or the indirect pathway, while fructose contributes only to the indirect pathway.

The AG carbons origin can be assessed by studying the position 1 via  $^{13}\text{C}$  NMR spectroscopy. This carbon has a singlet that corresponds to the 1.11% natural abundance  $^{13}\text{C}$  of this isotope, while the presence of multiply-labeled  $^{13}\text{C}$  fragments from metabolism of  $[\text{U-}^{13}\text{C}]\text{fructose}$  precursors (see Figure 5) will generate multiplet signals as a result of  $^{13}\text{C}$ - $^{13}\text{C}$ -coupling..

The  $^{13}\text{C}$  NMR spectrum of AG has better resolved signals compared to the  $^2\text{H}$  spectrum, in large part because  $^{13}\text{C}$  resonances have a much larger range of chemical shift dispersion (0-200 ppm) compared with  $^2\text{H}$  or  $^1\text{H}$  nuclei (0-12 ppm). The carbon-13 spectra of AG, shows signals at 101.0 ppm (C1), 73.4 ppm (C2), 76.1 ppm (C3), 72.3 ppm (C4), 76.5 ppm (C5) and 175.6 ppm (C6). In the case where the  $^{13}\text{C}$  spectrum has  $^{13}\text{C}$ - $^{13}\text{C}$ -coupled multiplets, i.e. following incorporation of  $[\text{U-}^{13}\text{C}]\text{glucose}$  into glucuronide, the multiplets of carbons 3 and 5 will partially overlap at fields of 14.1 T or less [20]. The  $^{13}\text{C}$  NMR spectrum of the MAGL derivative presents signals at 106.9 ppm (C1), 83.0 ppm (C2), 81.5 ppm (C3), 78.9 ppm (C4), 70.3 ppm (C5) and 174.2 ppm (C6). The signals are sufficiently dispersed such that there are no overlapping  $^{13}\text{C}$ - $^{13}\text{C}$ -coupled multiplets thereby enabling more reliable quantification of multiplet components for all six resonances.

## Dissertation objectives

The primary objective of this dissertation was to develop and optimize a purification technique that would avoid the derivatization of AG to MAG/MAGL/MAGLA. This process is not only laborious, but it also results in a significant loss of analyte that can severely reduce the signal-to-noise ratio of the NMR spectrum.

The approach being developed in this work is intended to be faster, easier and giving better yields particularly with small sample sizes such as those from mice. Based on the protocol described in Burgess et al. [19], the present study used DSC18 SPE-columns to purify and isolate the urinary AG.

This technique was then applied to mice animal models that were fed high sugar diets mimicking high intake of HFCS-55, (a mixture of 55% fructose and 45% glucose).

Using  $^2\text{H}$  and  $^{13}\text{C}$  stable isotope tracers mentioned previously, the goal is to study the contributions of different sources to hepatic glycogen synthesis. Deuterated water is delivered via intraperitoneal injection and drinking water, and  $^{13}\text{C}$ -tracers are provided by uniformly-labeled fructose and glucose ( $[\text{U-}^{13}\text{C}]$ fructose and  $[\text{U-}^{13}\text{C}]$ glucose) that are included in the sugar formulation.

To provide a non-invasive chemical biopsy, the animals are also administered with acetaminophen and AG is recovered from the urine. AG is then analyzed for  $^2\text{H}$  and  $^{13}\text{C}$  enrichment by  $^2\text{H}$  and  $^{13}\text{C}$  NMR, from this information, the contributions of various endogenous and exogenous substrates, including the glucose and fructose components are estimated.

# Methods

---

## [AG solubilisation in water](#)

Commercial acetaminophen  $\beta$ -D-glucuronide (Sigma-Aldrich) was dissolved in water. Each sample had approximately 3.49 mg of AG in order to achieve 10  $\mu$ mol in 1 mL of distilled water. This experiment was then concluded with  $^1\text{H}$  and  $^{13}\text{C}$  NMR acquisition, to make sure that 10  $\mu$ mol was enough AG to result in good NMR signals.

## [AG stability test](#)

1-2 mL of native human urine was spiked with commercial acetaminophen  $\beta$ -D-glucuronide and dissolved, with each sample having 10  $\mu$ mol of AG. Four samples were made and put under different temperatures: room temperature (sample A), refrigerated (sample B), refrigerated with a bacteriostatic agent sodium azide (sample C) and frozen (sample D). Sample A was checked periodically (0 h, 8 h, 24 h, 1 week, 2 weeks, 1 month and 6 months) and  $^1\text{H}$  NMR spectra was acquired.

Further studies for the stability, to acquire deuterium spectra, were performed later on. Two samples were put under high temperatures (50  $^{\circ}\text{C}$  and 65  $^{\circ}\text{C}$ ) for 24 h and then  $^1\text{H}$  NMR spectra were acquired to assess the stability of each one.

## [DSC-18 SPE columns](#)

The DSC-18 SPE columns work via Van der Waals interactions, meaning that the urine sample pH needs to be lowered to 2.0-2.5 to protonate the glucuronic acid moiety of the AG (since its pka is 3.21) and promote the bond between the molecule and the column. The pH cannot be lowered too much because there is a risk of hydrolyzing the glycosidic bond, between the glucuronic acid and the acetaminophen, that makes the AG.

## Urine spike with commercial AG

1-2 mL of native human urine was spiked with commercial acetaminophen  $\beta$ -D-glucuronide and dissolved, with each sample having 10  $\mu$ mol of AG.

The protocol described at Burgess et al. [19], was adapted by avoiding the use of urease (using acidic water to clear urea from the columns instead) and avoiding the derivatization steps.

0.5 mg/3 mL DSC-18 SPE columns were used and prepared with 3 mL of 100% methanol and 10 mL of acidic water (0.024% Trifluoroacetic acid, TFA). The sample had its pH lowered to 2-2.5 to promote the bind to the column, and was loaded into the column. The column was washed first with 4 mL of acidic water, then eluted with 3 mL of 10% methanol in acidic water, and a final wash with 2 mL of 100% methanol. The elution phase was collected into 5 fractions.

The results of this experiment were analysed through a colorimetric method using Cytation 3 Cell Imaging Multi-Mode Reader by BioTek Instruments, Inc. Because AG has an aromatic ring, it absorbs light, specifically at 295 nm after adding and also by  $^1\text{H}$  NMR spectroscopy.

## DSC-18 SPE column optimization

Using native human urine and spiking it with commercial AG, the same experiment was scaled up to 1 g/6 mL DSC-18 SPE columns, resulting in doubling all volumes.

The protocol was adapted using 1 g/6 mL DSC-18 SPE columns and maintaining the preparation phase (6 mL of 100% methanol and 20 mL of acidic water (0.024% TFA)), but adjusting the wash and elution volumes. The first wash was performed using 5 mL of acidic water (0.024% TFA) and the elution was performed with 4 mL of 10% methanol in acidic water. The final wash using 100% methanol was not performed, but the column was guarded if further studies were needed.

This experiment was concluded with  $^1\text{H}$  NMR spectra acquisition and analysis.

## Human administration of acetaminophen

A voluntary ingested orally 1 g of acetaminophen and the urine was collected at time stamps (0 h, 2 h, 4 h and 6 h), totaling 4 samples. A fraction of each sample was collected (approximately 30  $\mu$ L) and  $^1\text{H}$  NMR spectra were acquired to quantify the amount of AG present using a pyrazine standard. The results were then extrapolated to the total urine sample volume. The experiment was intended to be conducted with the amounts expected in mice (10  $\mu$ mol of AG in 1-2 mL of urine), so the human urine was adjusted to 10  $\mu$ mol by measuring the respective volume and adding distilled water to totalize 1 mL. In cases where the volume was greater than 1 mL, the sample volume was reduced using a Buchi R-200 Rotary Evaporator.

These samples were processed using the protocol described previously with 1 g/6 mL DSC-18 SPE columns.

The acidic water (washing phase) and 10% methanol in acidic water (elution phase) were collected and analyzed via proton NMR, with a pyrazine standard to assess the efficiency of this process in isolating and purifying AG.

After this experiment, the human samples mentioned were scaled up to human quantities and the protocol was adapted to use 10 g/60 mL DSC-18 SPE columns and the tenfold of all the volumes. The expected human quantities are variable between individuals, but average around 300-900  $\mu\text{mol}$  and 100-300 mL of urine. The volumes were adjusted using the same techniques mentioned for the 10  $\mu\text{mol}$ /1-2 mL urine samples, but to the adequate volumes.

## Mice

The laboratory mice used (C57BL/6) were susceptible do diet-induced obesity and type 2 diabetes. Twenty-one male mice that were 8 weeks old and housed three to a cage were divided into three groups (A, B and C) for the diet trials. Within each group, some mice were maintained as control (Teklad Diet, without sugar added to the drinking water), while other mice groups were submitted to a HS where they had normal chow supplemented with 55/45 mixture of fructose and glucose, as to mimic HFCS-55, totalling 30% of the drinking water mass.

The groups were fed these diets for 16-18 weeks. Three days before sacrificing the mice, they were moved into a metabolic cage (Figure 7), 3 days for acclimatization and the last dark cycle on the third day for the metabolic study. The relatively long period of acclimatization is because of the environmental change, that usually increases the stress levels. While they were provided with cardboard “igloo” structure where they could hide, in the metabolic cage there are no hiding spots. The other source of stress is the inability for the mice to socialize in the metabolic cage. While normally there are 3-4 animals sharing a cage, in the metabolic cage they are alone. The animal is placed in the top compartment, as seen in Figure 7 with free access to food and drinking water. Both faeces and urine go down through the funnel placed bellow. On the bottom of the funnel there is a plate that separates the solid (faeces) from the liquid (urine), and stores the urine into a cup.

On the start of the dark period of the third day, the glucose/fructose mixture in the drinking water was substituted by identical mixtures where each sugar was enriched with  $^{13}\text{C}$  and were divided into two groups: HS1 (group with high sugar diet, with 20% [U- $^{13}\text{C}$ ]glucose labelling) and HS2 (group with high sugar diet, with 20% [U- $^{13}\text{C}$ ]fructose labelling).

At the start of the dark period, mice of all three groups received an intraperitoneal injection of 99.9% deuterated water (4 g/100 g body weight) in which 10 mg/100 g body weight of acetaminophen had been dissolved and the drinking water was supplemented with 5% deuterated water. Each mouse was allowed to feed naturally overnight and its urine was collected over this period, and the urine was collected for posterior purification using a DSC-18 SPE column, and subsequent  $^2\text{H}$  and  $^{13}\text{C}$  NMR analysis.

This thesis is inserted in a bigger project. The mice protocol and its procedures were performed by other scientists. The author of this thesis did not partake in the experiments mentioned above.



Figure 7- Tecniplast™ Metabolic Cage for single mouse.

## Acetaminophen-glucuronide hydrolysis

AG was hydrolysed into glucuronic acid and paracetamol. The followed protocol is an adaptation of the one described in Jones et al. [20], specifically a scale down from human to mice amounts. The 10% methanol in acidic water phase (elution phase) resulting from the DSC-18 SPE column purification process was evaporated to dryness. This residue was re-suspended in 5-8 mL of distilled water and the pH was adjusted to approximately 4.5 by adding a low concentration solution of sodium hydroxide (0.5 and 0.25 molar). For the hydrolysis of acetaminophen-glucuronide, 200 units of  $\beta$ -glucuronidase (Sigma Chemical Company) were added and the solution was incubated at 40 °C for 72 h. The solution was then passed through 1 mL of Dowex™ 50WX8 100-200 resin [20]. The purified solution was collected and evaporated to reduce the volume, but without reaching complete dryness and avoiding the formation of the lactone.

The same procedure was applied to some human samples. The residue was re-suspended in 40-50 mL of distilled water and the pH was adjusted the same way mentioned previously. The hydrolysis was performed with 2000 units of  $\beta$ -glucuronidase (Sigma Chemical Company) followed by incubation at 40 °C for 72 h. The solution was then passed through 3 mL of Dowex™ 50WX8 100-200 resin [20]. The purified solution was collected and evaporated to reduce the volume. This specific resin has a 50-58% water retention capacity and contains 8% of a copolymer of styrene and divinylbenzene that confers the resin with maximum resistance to oxidation, reduction, mechanical wear and breakage [45]. This will filtrate all the salts and ions from the pH adjusting step and the enzymatic reaction with the glucuronidase.

Some samples were evaporated to dryness to follow to MAGL derivatization.

## Glucuronic acid derivatization to MAGL

The derivatization of glucuronic acid to MAGL was adapted from Jones et al. [20]. A solution containing 5 mL of deuterated acetone and 10  $\mu$ L of deuterated sulphuric acid was prepared. The solution was stirred for 5-10 minutes and refrigerated for an equal period of time. After that, 5 mL of the solution were added to each sample with glucuronic acid (after 72 h of incubation of the sample with the enzyme  $\beta$ -glucuronidase). The mixture was stirred for 24 h, after which 5 mL of distilled water were added and the pH of the sample was adjusted to 4.5-5 with 1 molar and 0.25 molar  $\text{Na}_2\text{CO}_3$ . Usually 1 mL of 1 M  $\text{Na}_2\text{CO}_3$  raises the sample pH to approximately 3.5. After that, small increments of 0.25 M  $\text{Na}_2\text{CO}_3$  were added until the pH reached 4.5-5.0 (approximately 200-400  $\mu$ L). The sample was then evaporated to dryness using a Genevac evaporator. At this point, MAGL is formed and all that is left is to isolate it from other compounds.

The same hydrolysis was executed in the human samples mentioned previously in the scale up of mice AG and urine volumes quantities to test the DSC18 SPE-columns efficiency in isolating AG. The sample was re-suspended in 40 mL of distilled water and its pH was adjusted to 4.5 by adding a low concentration of sodium hydroxide (0.25 molar). The AG was hydrolysed using 2000 units of  $\beta$ -glucuronidase, for the same period of time and at the same temperature as for the mice samples. The solution was then passed through 3 mL of Dowex<sup>TM</sup> 50WX8 100-200 resin [20]. The purified solution was collected and evaporated to reduce the volume.

The residue was re-suspended using 1 mL of acetonitrile (for mice samples) and 2 mL of acetonitrile (for human samples). Because the pellet is very dry, it is required to scrape off the residue from the interior of the glass balloon. The re-suspended solution is transferred into an Eppendorf. Some parts of the residue does not dissolve and cannot be transferred using the pipette, but instead using a spatula. The Eppendorf is centrifuged at 7000 rotations per minute for approximately 5 minutes. The supernatant is collected into a different Eppendorf and the acetonitrile is evaporated in a fume-hood at room temperature for 84 hours.

A DSC-18 SPE column purification protocol followed. 500 mg/3 mL columns were prepared using 3 mL of acetonitrile and 10 mL of acidic water (pH higher than 4.5). The pellet was re-suspended with 200  $\mu$ L of acidic water and loaded into the column a total of three times. The column was washed with 1 mL of acidic water and eluted with 2 mL of a mixture of 80% acidic water and 20% acetonitrile. The elution phase was collected. The acetonitrile was evaporated using the hotte at room temperature for 24 hours, and the water was evaporated using a lyophilizer or Genevac evaporator.

Human urine samples (after administration of acetaminophen and deuterated water to achieve 0.5 % body water deuterium enrichment) containing AG were also derivatized to MAGL. The protocol was a scale up of the one mentioned immediately above using DSC-18 SPE columns of 2 g/ 12 mL. All the volumes augmented 4 times: 12 mL and 40 mL of acetonitrile and acidic water, respectively

for the column preparation, 800  $\mu\text{L}$  of acidic water to re-suspend the pellet, 4 mL of acidic water to wash the sample through the column and finally 8 mL of the 20% acetonitrile in acidic water.

## NMR experiments

### Proton- $^1\text{H}$

$^1\text{H}$  NMR spectra of AG samples were obtained at 25  $^{\circ}\text{C}$  with a 9.4 T with a Bruker Avance III HD Unity 400 system equipped with a 5 mm broadband probe ( $^1\text{H}$  operating frequency 400MHz). For  $^1\text{H}$  acquisition, a spectral width of 6 kHz (15 ppm), 90-degree pulse angle, 5.45 s acquisition time and 5 s interpulse delay were used with 32768 points acquired. Each  $^1\text{H}$  spectrum was acquired with 16 free-induction decays (FID).

### Deuterium- $^2\text{H}$

The dried sample was re-suspended with 450  $\mu\text{L}$  of 99% deuterium depleted water and it was added 25  $\mu\text{L}$  of pyrazine standard and 50  $\mu\text{L}$  of hexafluoroacetone for the lock capture. The  $^1\text{H}$  pyrazine peak intensity was compared with the AG methyl peak to make its quantification.

Plasma body water  $^2\text{H}$ -enrichments were determined from 30  $\mu\text{L}$  of human urine samples/ 10  $\mu\text{L}$  of mice urine samples by  $^2\text{H}$  NMR as described by Jones et al. [46]. This study used 30 $\mu\text{L}$  of sample, 1 mL of acetone (assuming the acetone weight 791 mg, the correspondent of 1 mL [46]) and 50  $\mu\text{L}$  of hexafluorobenzene for capture lock. The ratio between the water peak area and the acetone peak gives the plasma body water  $^2\text{H}$ -enrichment (in percentage if the ratio is multiplied by 100). This value can be normalized by using a constant multiplying it to the ratio of the acetone weight and the sample weight.

Proton-decoupled  $^2\text{H}$  NMR spectra of AG samples were obtained at 25  $^{\circ}\text{C}$  with a 11.7 T ( $^1\text{H}$  operating frequency 500MHz) with a Bruker Avance III HD equipped with an UltraShieldPlus<sup>TM</sup> magnet, with a 5 mm selective probe with  $^1\text{H}$ -acquisition/decoupling coil and  $^{19}\text{F}$  lock.

Spectra were obtained with a 90 $^{\circ}$  pulse angle, an acquisition time of 2.2 seconds (2048 data points), a sweep width of 77 MHz (10 ppm), and a pulse delay of 0.1 seconds. Number of acquisitions approximately 28.700 (18 h). The summed free induction decays were processed with 0.5-1.0 Hz line-broadening before Fourier transform.

Deuterium spectra acquisition was optimized by promoting ppm shift to isolate the signal 5 from the water signal. Two separate experiments were done: adding trifluoroacetic acid (TFA) and adding a mixture of 10% acetonitrile in distilled water.

AG  $^2\text{H}$ -enrichments were quantified from the  $^2\text{H}$  NMR spectra by measuring the area of each signal of the AG hexose moiety (1 to 5) relative to the peak area of the reference pyrazine signal at 8.6



ppm. Spectra were analysed with the NUTS Pro™ PC-based NMR spectral analysis software (Acorn NMR Inc., USA).

The relative contributions of the direct and indirect pathways were calculated with equations 1 and 2, where H5 corresponds to the deuterium enrichment found in the position 5 of the AG.

Equation 1

$$\text{Indirect pathway contribution (\%)} = 100 \times \frac{H5}{\text{body water } ^2H \text{ enrichment}}$$

Equation 2

$$\text{Direct pathway contribution (\%)} = 100 \times \left(1 - \frac{H5}{\text{body water } ^2H \text{ enrichment}}\right)$$

Carbon-13- <sup>13</sup>C

Proton-decoupled <sup>13</sup>C NMR spectra were acquired at 14.1 T with a Varian600 spectrometer equipped with a 3-mm broadband “switchable” probe with z-gradient (Varian, Palo Alto, CA). Spectra were obtained with a 90° pulse angle, an acquisition time of 4.3 seconds (131072 data points), a sweep width of 30 KHz (200 ppm), and a pulse delay of 0.5 seconds. The number of acquisitions were 32,000.

The WALTZ-16 decoupling sequence was used for proton decoupling of both <sup>2</sup>H and <sup>13</sup>C. <sup>2</sup>H free induction decays (FIDs) were multiplied by an exponential function corresponding to 0.5 to 1.0 Hz line-broadening before Fourier transform while <sup>13</sup>C FIDs were processed with 0.1 to 0.5 Hz line broadening. The relative areas of <sup>13</sup>C NMR multiplets were quantified using the curve-fitting routine supplied with the NUTS Pro™ PC-based NMR spectral analysis software (Acorn NMR Inc., USA).

The relative contributions of the direct and indirect pathways were calculated with equations 3 and 4. [U-<sup>13</sup>C<sub>6</sub>]AG is the carbon-13 enrichment found in AG, and [U-<sup>13</sup>C]glucose corresponds to the percent of uniformly labelled glucose enrichment added in the chow. For the indirect pathway contribution (equation 4), it is considered that [1,2-<sup>13</sup>C<sub>2</sub>]AG and [5,6-<sup>13</sup>C<sub>2</sub>]AG, [1,2,3-<sup>13</sup>C<sub>3</sub>]AG and [4,5,6-<sup>13</sup>C<sub>3</sub>]AG are equivalent isotopomers, correspondingly. The 1.5 factor accounts for carbon-13 tracer dilution by the Krebs cycle and is based on the assumption that net anaplerotic outflow is approximately 2-fold that of Krebs cycle oxidative flux.

Equation 3

$$\text{Direct pathway} = 100 \times \frac{[U-^{13}C_6]AG \text{ enrichment}}{[U-^{13}C]glucose \text{ enrichment}}$$

Equation 4

$$\text{Indirect pathway} = 100 \times 1,5 \times \frac{[1,2-^{13}\text{C}_2]\text{AG} + [1,2,3-^{13}\text{C}_3]\text{AG enrichments}}{[\text{U-}^{13}\text{C}]\text{glucose enrichment}}$$

It is assumed that the fructose was metabolized entirely by the indirect pathway.

# Results and Discussion

## DSC-18 SPE column protocol development

### AG initial experiments and stability tests

The first step of this study was to assess if the expected AG mice quantity excreted in urine (~10  $\mu\text{mol}$ ) would be enough to acquire quality  $^2\text{H}$  and  $^{13}\text{C}$  NMR spectra. Commercial AG was dissolved in distilled water to reach the concentration of 10  $\mu\text{mol}$  of AG.  $^1\text{H}$  and  $^{13}\text{C}$  NMR spectra were acquired (Figure 6 and Figure 8).

The spectrum shown in Figure 8 reflects the dissolved commercial AG with the positions 1-6 numbered (101.0 ppm; 73.4 ppm; 76.1 ppm; 72.3 ppm; 76.5 ppm and 175.6 ppm respectively, in numerical order from 1 to 6). While the carbon-13 spectra has signal for the position six, the proton spectra does not, because the carbon 6 is part of a carboxyl group, hence not having a proton signal. The peak at 154.3 ppm corresponds to the aromatic ring carbon bond to the oxygen which is part of the glycosidic bond between the acetaminophen and the glucuronide, 132.1 ppm is the peak of the aromatic ring carbon bond to the nitrogen, 124.2 ppm and 117.3 ppm are the carbons at the meta and ortho positions, respectively, in relation to the carbon responsible for the glycosidic bond. The carbonyl group has a  $^{13}\text{C}$  NMR peak at 173.4 ppm and the methyl group at 22.5 ppm.

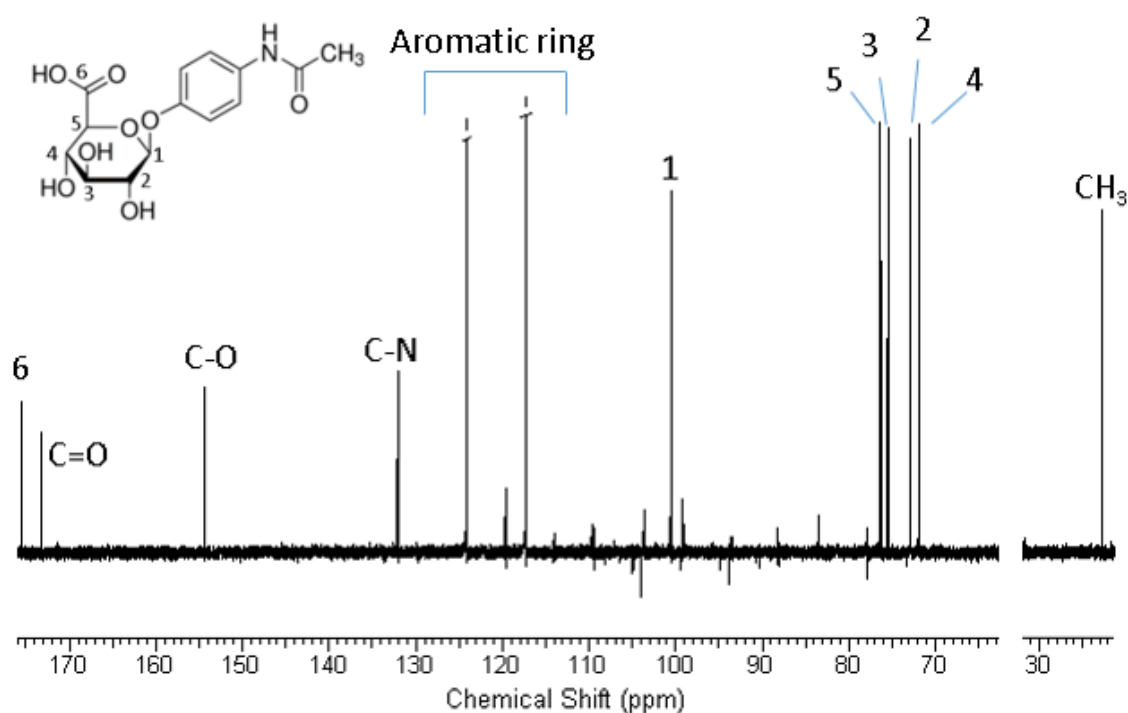


Figure 8-  $^{13}\text{C}$  NMR spectra of 10  $\mu\text{mol}$  of commercial AG dissolved in 1-2 mL of distilled water with the numbered carbons of the glucuronide.

NMR experiments can be conducted under high temperatures to promote ppm shifts and isolate some peaks, and/or with a chemical environment that differs from the optimal for the sample in use. Both these parameters can lead to AG degradation, so it was required to perform stability tests under the conditions mentioned above. One factor to take in account is that there might be a large period of time between the sample collection and the NMR spectra acquisition. For this reason is important for the sample to remain intact through that period of time, therefore being also important to study its stability over time.

The expected mice urine volume and AG excretion were mimicked by spiking native urine from a human voluntary with commercial AG. Four samples were made and put under different temperatures: room temperature (sample A), refrigerated (sample B), refrigerated with a bacteriostatic agent sodium azide (sample C) and frozen (sample D). Sample A was checked periodically (0 h, 8 h, 24 h, 1 week, 2 weeks, 1 month and 6 months) and  $^1\text{H}$  NMR spectra was acquired at those time stamps. None of the spectra of the sample A showed any signs of degradation, so the remaining samples (B, C and D) were never tested.

Further studies for the stability, to acquire deuterium spectra, were performed later on. Spiking a native human urine sample with commercial AG. The sample was put under high temperatures (50 °C and 65 °C) for 24 h and then  $^1\text{H}$  NMR spectra were acquired to assess the stability. No signs of degradation were observed in any of the samples (Figure 9). This experiment used pyrazine standard referenced at 8.63 ppm. The signals from the aromatic ring (between 7.10 and 7.35 ppm), the signal from the methyl group (2.15 ppm) and the signal H1 (5.10 ppm) are similar in all 3 spectra, providing proof that the high temperature is not promoting sample degradation. Some peaks present ppm shift, moving to higher ppm's (lower field) with higher temperatures. Although some spectra showed the signal H5, that would further confirm the absence of sample degradation, other spectra did not have a quality signal to be comparable with each other therefore this peak being absent in the Figure 9.

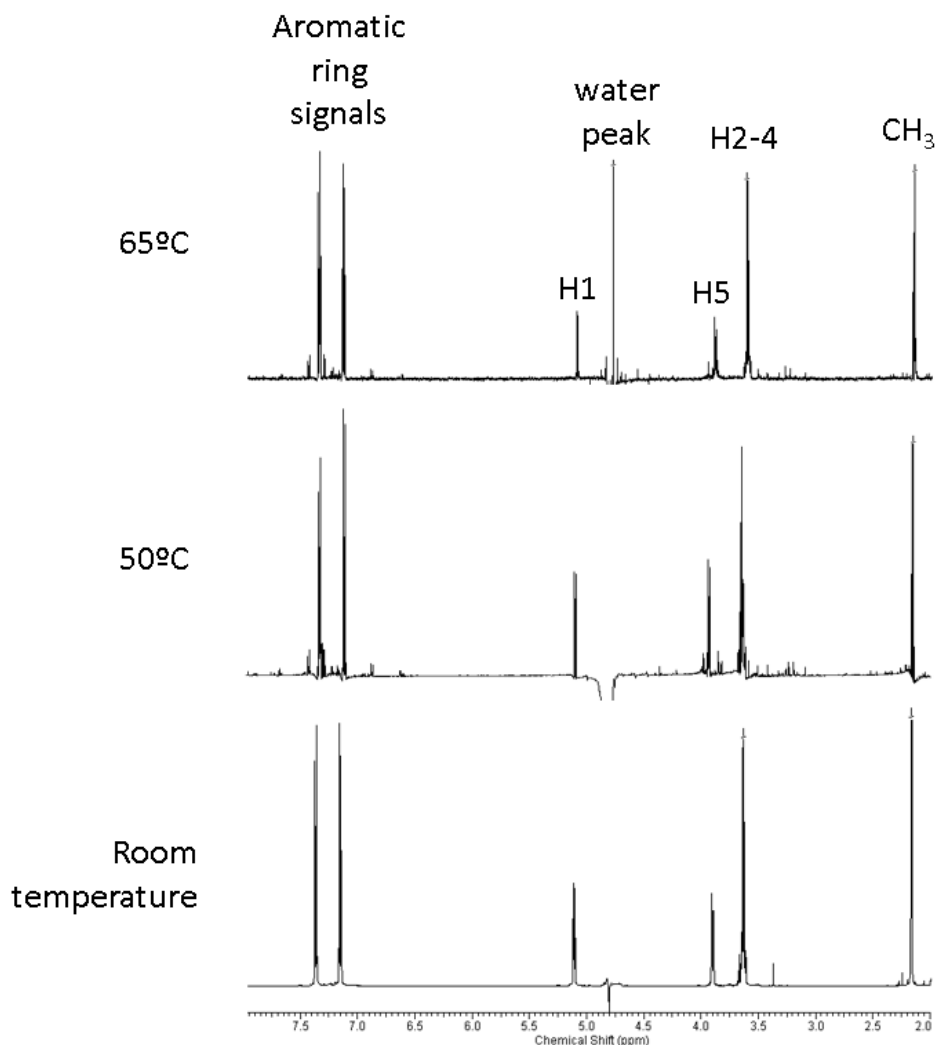


Figure 9-  $^1\text{H}$  NMR spectra of AG samples under different conditions: room temperature (native elution sample), 50 °C (elution sample put under 50 °C for 24 h previously to the  $^1\text{H}$  NMR experiment) and 65 °C (elution sample put under 65 °C for 24 h previously to the  $^1\text{H}$  NMR experiment). The several spectra shown are not at the same scale.

### [DSC-18 SPE columns protocol development and optimization](#)

The column preparation is based on a protocol described on Burgess et al. [19] as part of a protocol for DSC-18 SPE columns. This type of columns are silica based, and are characterized for having narrow spaces that allow molecules to bind to the silica. Such characteristics make this column a perfect choice to separate drugs (because of their small size) from aqueous solutions. Another factor to take into account is that this columns work in reversed-phase. Among others, Van der Waals interactions are in this category.

AG has a more polar side (the glucuronic acid moiety of the molecule) and a more apolar side (the acetaminophen moiety of the molecule). The last referred part will interact with the silica polymer through hydrophobic interactions, in other words, the more apolar part of the AG will bind to the column.

To prepare the column the standard procedure is to use water to wet the column and remove any impurities, followed by methanol that penetrates the narrow gaps in order to prepare the column to receive the sample. These two solvents (water and methanol) are specific because they are the ones that are going to be used: to wash the column acidic water, that will wash all the polar analytes; and to elute the column 10% methanol in acidic water, that will unbind the AG from the column, without changing the polar environment.

The low pH of the water and 10% MeOH are justified because of the acidic nature of the sample that is going to be loaded in the column, even though pH was lowered even further to promote the Van de Waals interaction of the molecule with the column [47]. The acidic water is an attempt to replace the use of urease as described in Burgess et al. [19] to wash the urea. Urease is used to decrease the sample density, easing the passage of the sample through the column and the purification of the sample. This step requires pH maintenance, since urease only works at low pH and as it reacts with urea, the pH tends to go up, inhibiting this enzyme. The way to keep this reaction going for long enough to lower the sample density is by slowly adding acid. In theory this is the optimal way to deal with urine samples in DSC-18 SPE columns, but maintaining and controlling the pH in samples averaging 1-2 mL is difficult.

In a first approach to this protocol 0.5 g/3 mL DSC-18 SPE columns were used. They were prepared with 3 mL of 100% methanol and 10 mL of acidic water (0,024% TFA). A urine sample spiked with commercial AG had its pH lowered to 2-2.5 using TFA to promote the bind to the column, and was loaded into the column. The column was then washed first with 4 mL of acidic water, eluted with 3 mL of 10% methanol in acidic water, followed by a final wash with 2 mL of 100% methanol. To assess when the AG was disconnecting from the column, the elution phase was divided into 5 fractions of approximately equal volume.

The results of this experiment were analysed through a colorimetric method using Cytation 3 Cell Imaging Multi-Mode Reader by BioTek Instruments, Inc. Because AG has an aromatic ring in the acetaminophen moiety of the molecule, it absorbs light, specifically at 295 nm (Figure 10).

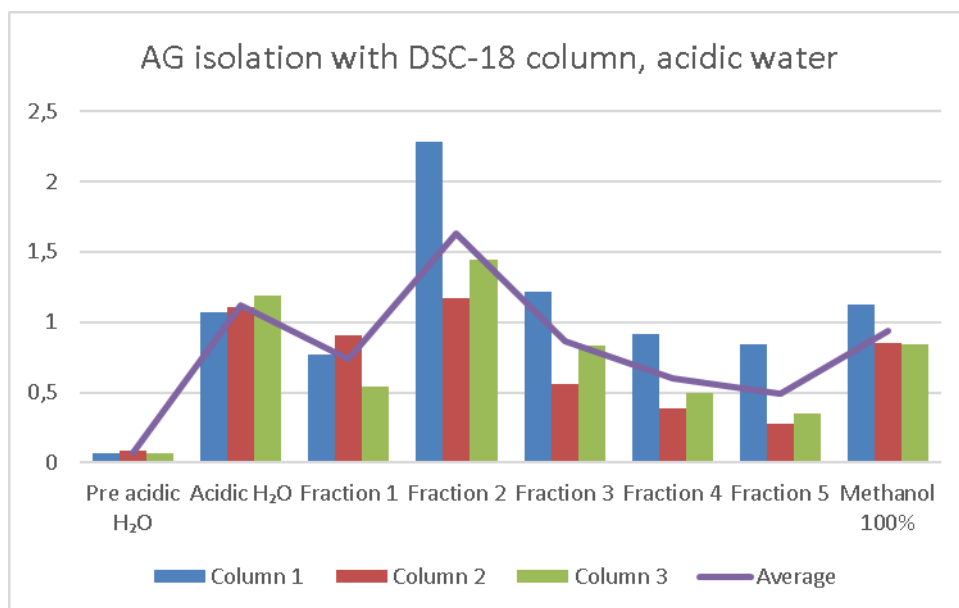


Figure 10 - Graphical representation of the colorimetric results of the purification of AG using DSC-18 SPE column. Each sample was made in triplicate and is represented with different colours. Loading volumes (pre-acidic H<sub>2</sub>O), first washing phase (acidic H<sub>2</sub>O), elution with 10% methanol (fraction 1 to 5, averaging 1 mL per fraction) and final washing phase (100% methanol). The purple line represents the average value for each phase.

As the Figure 10 shows, most of the AG binds to the column, since the “pre-acidic H<sub>2</sub>O” phase has a very low absorbance. This means that there is little to no AG being disconnected from the column. The absorbance being higher than zero is justified by the urine having aromatic compounds that might not bind to the column and are immediately released.

The first wash collection shows a higher absorbance and the results are common for all the 3 columns. The absorbance intensity is similar for both the first and final wash, with acidic water and 100% methanol, respectively. Although the elution fractions show a curve that indicates that the AG is disconnecting from the column progressively.

The overall conclusion is that there is either a lot of AG being washed away with acidic water, or that other compounds present in the urine also have an absorbance at 295 nm and are interfering with the plate-reading experiment (false positive).

To clarify what was happening in the column, the fractions of both the wash phases and the elution phase were also analyzed through <sup>1</sup>H NMR spectroscopy. This experiment showed approximately 30% of AG disconnecting from the column with the first wash (acidic water), 70% of AG present in the elution phase (10% methanol in acidic water), and no traces of AG in the final wash using 100% methanol. This experiment was made in triplicate.

Figure 11 shows three of the <sup>1</sup>H NMR spectra obtained from this experiment. Peak A corresponds to the pyrazine standard used is observed at 8.5 ppm in all spectra (A, B and C). The A spectrum is relative to the wash phase with acidic water and there is present several urine metabolites, such as urea, creatinine and glycine, between 2.5 and 4.25 ppm. This is the range at which the signal 5 (H5) from the AG appears.

The B spectrum corresponds to the elution phase with 10% methanol in acidic water. When comparing A and B spectra, it is clear that most of the urine metabolites were washed away and that the B spectrum is relatively pure and has the peak of interest (H5) isolated from any other signals. Furthermore, the peaks H2-4 from the glucuronide moiety are also observable in this spectrum, but they are overlapped as explain previously. Nonetheless, this agglomeration of peaks is also isolated, which indicates a purified sample.

The C spectrum is the final wash with 100% methanol. The AG quantification is made by using a pyrazine standard and comparing to the methyl group peak (2.1 ppm). In other words, the methyl group peak area is directly proportional to the amount of AG present in the sample. In the C spectrum there is no methyl group signal, which means that there is no AG in the last wash. Most peaks are from urine metabolites, like the aromatics compounds.

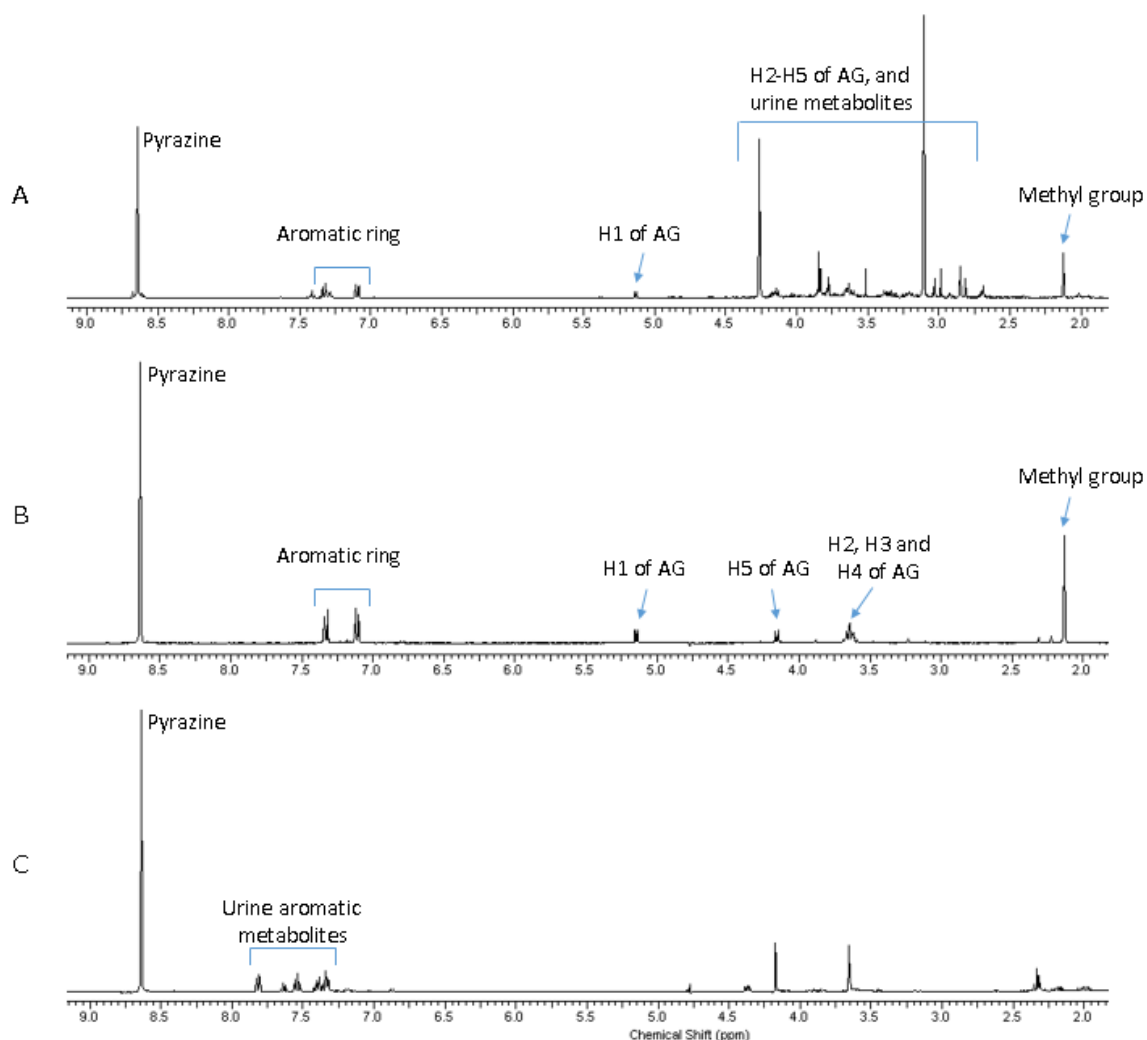


Figure 11-  $^1\text{H}$  NMR spectra from the results of using a SPE-column to purify AG from urine obtained after spike with commercial AG. H1 to H5 refers to the protons of the glycosidic moiety of the AG. First wash phase using acidic water (A), elution phase using 10% methanol in acidic water (A), elution phase using 10% methanol in acidic water (B), and a final wash phase with 100% methanol (C).



Knowing that the last wash presents no detectable AG signals, it is safe to assume that 100% of the acetaminophen-glucuronide is in the first wash and the elution, disregarding the possibility that some small amount of AG stood in the column.

The quantification of the methyl peaks of the spectra acquired yielded an average of 70% AG in the elution phase and 30% in the first wash. Although 70% of purified and isolated AG is a higher yield than the derivatization protocols mentioned before, it was intended for this process to have an even higher efficiency.

Further tests to improve the DSC-18 SPE column efficiency were performed in 1 g/6 mL columns, since they were more suitable to the AG amounts and urine volumes expected from mice samples. Lowering the urine sample pH even further to promote the bind between the molecule and the column was hypothesised as a solution, but the low pH could potentially break the glycosidic bond between the glucuronic acid and the acetaminophen. This was an unviable solution.

A potential problem with this process might have been due to column bind competition. The acidic water could be competing with the AG for the bind to the column. This idea was tested by undergoing the same protocol as before, but with water at a higher pH (approximately 7). Figure 12 shows that both the acidic water and the neutral pH water had similar results through all the experiments, meaning that this was not the problem either.

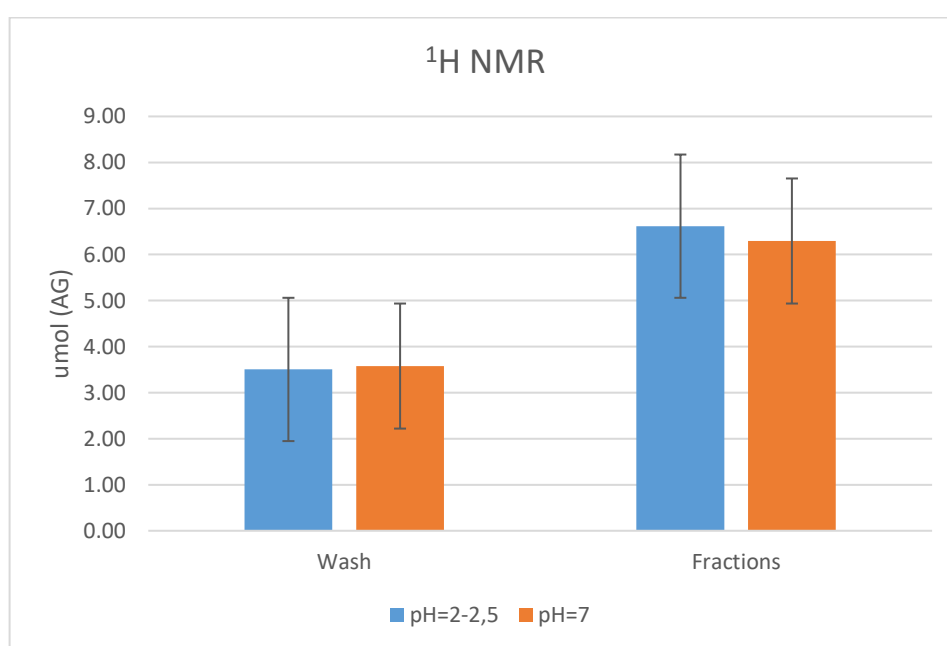


Figure 12- Graph comparing the efficiency of using water with different pH (2.5 and 7 coloured with blue and orange, respectively) to wash the native human urine sample spiked with commercial AG in DSC-18 SPE columns.

Still on the train of thought that the 70% AG in the elute could mean a column bind competition in the washing phase prior, it was used a second column to purify some of the 30% AG lost in the washing phase of the first column. The protocol used for both columns was the same as described previously. The first column was prepared, loaded with a urine sample, washed and eluted. The

second column was prepared, loaded with the collected washing phase from the first column, washed and eluted. The results showed that only 6% of AG was recovered in the elution phase of the second column, totaling 76% of AG being purified (70% on the first column and 6% on the second column). It is a better result than the first one (70%), but the slight increase in performance by 6% does not justify the use of a second column.

As a last resort to improve the efficiency of this process, the volume of acidic water used to wash the sample was reduced from 8 mL to 5 mL. The idea here was that the acidic water was probably saturating the column. Since Van de Waals interactions are very weak and using too much solvent could lead to some of the AG to simply disconnect from the column. Several experiments were performed using this protocol, and resulted in better recoveries of AG (shown below).

In short, the lastly developed protocol consisted in a 1 g/6 mL column preparation with 6 mL of 100% methanol followed by 20 mL of acidic water (0.024% TFA). The sample pH was lowered to 2-2.5 using TFA and loaded into the column. The column was washed with 5 mL of acidic water (0.024% TFA) and eluted with 10% methanol in acidic water. The final wash with 100% methanol was discarded since many experiments were performed and none showed traces of AG.

TFA was the chosen acid because of its high volatility. Since TFA is easily evaporated, it is safe to assume that when the elution fraction is dried and re-suspended into a NMR tube, there will not be any TFA present. This way there will be no interference in the chemical environment while acquiring NMR spectra causing ppm shifts or sample degradation.

Acetaminophen administration experiments followed. A voluntary took 1 g of acetaminophen orally with the interest of closing the gap towards the expected results from an animal model. Urine samples were collected at time 0-2 h, 2-4 h and 4-6 h.

The protocol described was performed using human samples that were scaled down to mice quantities (10  $\mu$ mol in 1-2 mL of sample). All the samples were quantified using  $^1\text{H}$  NMR spectroscopy. The methyl peak area was determined and used to quantify the amount of AG present in the sample, as explained in "Methods".

It is expected that the  $^1\text{H}$  NMR spectra have AG, acetaminophen-sulphate (AS) and free acetaminophen (A) [48]. Figure 13 shows part of the  $^1\text{H}$  NMR spectra acquired from the sample obtained at the 2 h timestamp, and the acetaminophen metabolites mentioned before.

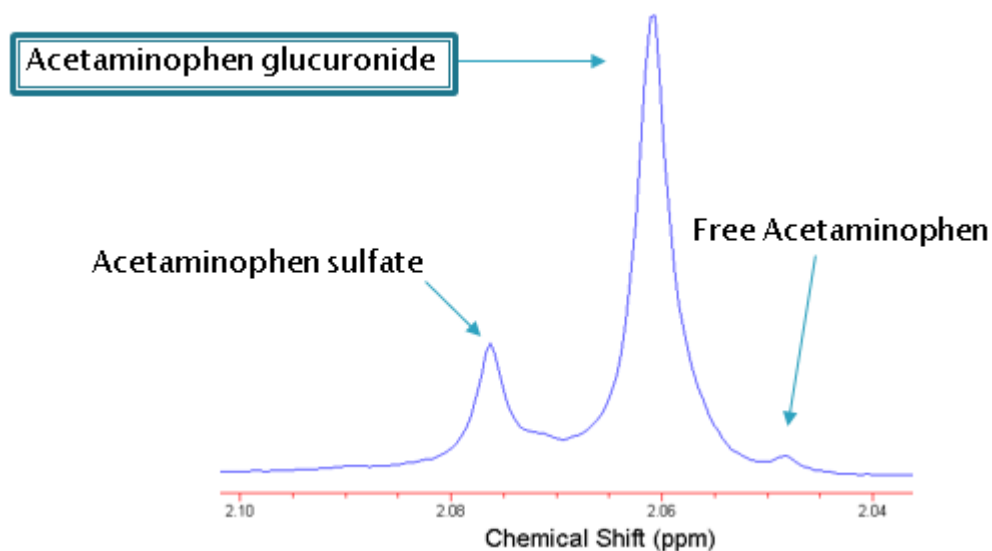


Figure 13-  $^1\text{H}$  NMR spectra of the 10% MeOH elution of the 2-4 h human urine sample.

The administration of acetaminophen, contrary to spiking the urine, results in more than one acetaminophen metabolite derivative. In fact, as mentioned previously, the administration of acetaminophen results in three components (AG, AS and free acetaminophen). All of them have an aromatic ring provenient from the acetaminophen moiety of the molecule. This results in all of the molecules mentioned absorbing at 295 nm, precluding the quantification of AG separately from the other two compounds. These can be resolved by  $^1\text{H}$  NMR spectroscopy, as shown in Figure 13.

The acidic water (washing phase) was collected and analyzed via  $^1\text{H}$  NMR, with a pyrazine standard. None of the wash collections showed any detectable signals from AG.

The 10% methanol in acidic water (elution phase) was also collected and analyzed using a pyrazine standard. This experiment was made in duplicate for each timestamp sample and showed approximately 84.2% and 64.0% (sample collected at 0-2 h), 85.5% and 78.9% (collected at 2-4 h), 73.4% and 108.8% (collected at 4-6 h) of AG yields. Disregarding the values of 64.0% and 108.8% (assuming a quantification error), on average  $80.5\% \pm 5.6\%$  of AG was being purified and isolated using this protocol.

The protocol used previously was scaled up to human amounts: 10 g/60 mL DSC-18 SPE columns instead of 1 g/6 mL, and all the volumes were also scaled up ten-fold. This experiment also relied on the  $^1\text{H}$  NMR quantification using the methyl peak area integration.

Similar results for the first washing phase when compared to the previous experiments, with no traces of AG. The elution phase showed recovery rates of approximately 85.89%, 91.86% and 91.69%. On average,  $89.81\% \pm 3.4\%$  of AG is isolated using this protocol adapted to human quantities.

To provide some clarity, the samples that showed  $80.5\% \pm 5.6\%$  and  $89.8\% \pm 3.4\%$  of AG recovery yields were sourced from human samples, with AG amounts higher than 100  $\mu\text{mol}$  and urine

volumes greater than 100 mL. Those samples were quantified using  $^1\text{H}$  NMR spectroscopy, as explained previously, and were adapted to mice and human quantities. The human quantities mentioned cannot be the whole sample since the higher capacity DSC-18 SPE columns available are 10 g/ 60 mL. The adaptation of the human samples to “human quantities” is required in order to not saturate those columns.

Mice quantities corresponds to 10  $\mu\text{mol}$  in 1-2 mL of sample and are loaded into 1 g/6 mL DSC-18 SPE columns. Human quantities corresponds to 100  $\mu\text{mol}$  in 100 mL of sample and are loaded into 10 g/ 60 mL DSC-18 SPE columns.

In summary, the newly developed protocol in this thesis that uses DSC-18 SPE columns to purify urine samples in order to study hepatic glycogenesis, shows an overall AG recovery of approximately  $85.16\% \pm 4.5\%$  and can be done in approximately 8 hours, instead of 20-45% yields using a protocol that needs approximately 2 weeks to be complete, as it happens in the derivatization process [20].

It is also important to assess the purity of the fraction obtained from the elution with 10% MeOH. In scope of this study, where there is a focus on the hepatic glycolytic flux, the  $^2\text{H}$  enrichment in the position 5 is the most important. Figure 14 shows the  $^1\text{H}$  NMR of the 4 mL collected on the elution phase with 10% methanol in acidic water which presents itself with high purity and in a well resolved manner, showing that the purification protocol is efficient. This is the intended result, and shows that the column is doing the expected: bind specifically to AG and not to other substances, allowing its separation and purification. Although the signals 2, 3 and 4 are overlapping and are not available to be studied and quantified, the signal 5 is well resolved and isolated.

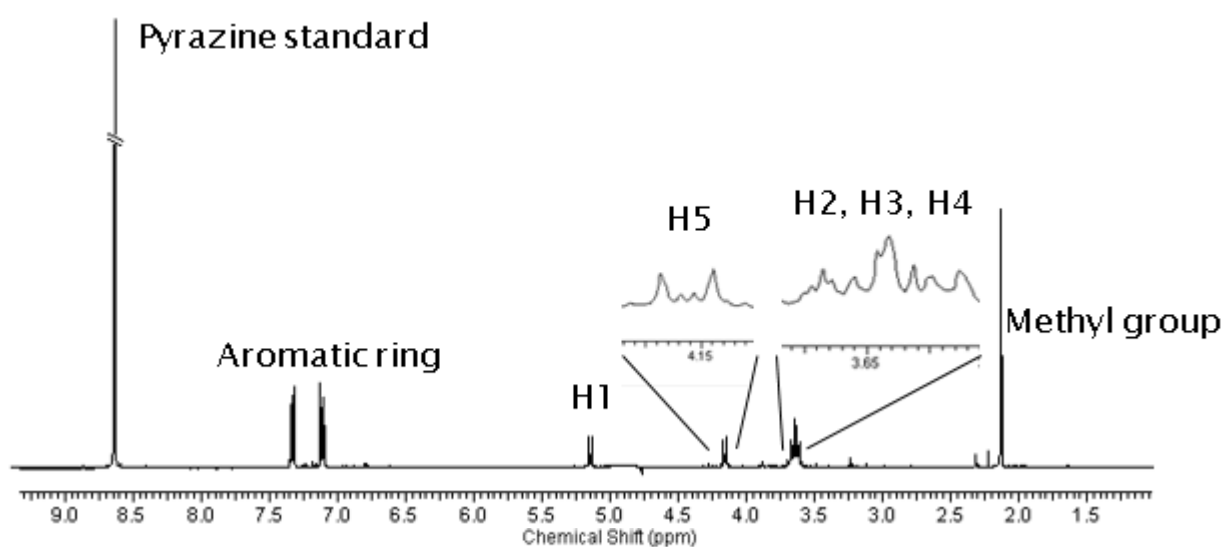


Figure 14-  $^1\text{H}$  NMR spectra of the column elution of urine sample with 4 mL of 10% methanol in acidic water. H1 to H5 refers to protons of the glycosidic moiety of AG.

## $^2\text{H}$ and $^{13}\text{C}$ spectra acquisition: tests and optimization

All that remains is to acquire  $^2\text{H}$  spectra and study the viability of the signal 5 (H5), as well as  $^{13}\text{C}$  spectra. As said before, it is important that this signal is isolated from all the others so it can be quantified. Figure 15 shows that the H5 could potentially be too close to the water signal. Moreover, the  $^2\text{H}$  signals of AG are broad, with linewidths of approximately 3.13 Hz for signals 1 and 5, and 8.17 Hz for the overlapping peaks (2, 3 and 4). These results were unexpected and are yet to be fully understood. It is thought that one of the main reasons for such broad signals could be the solvent used, even though AG is very soluble in water.

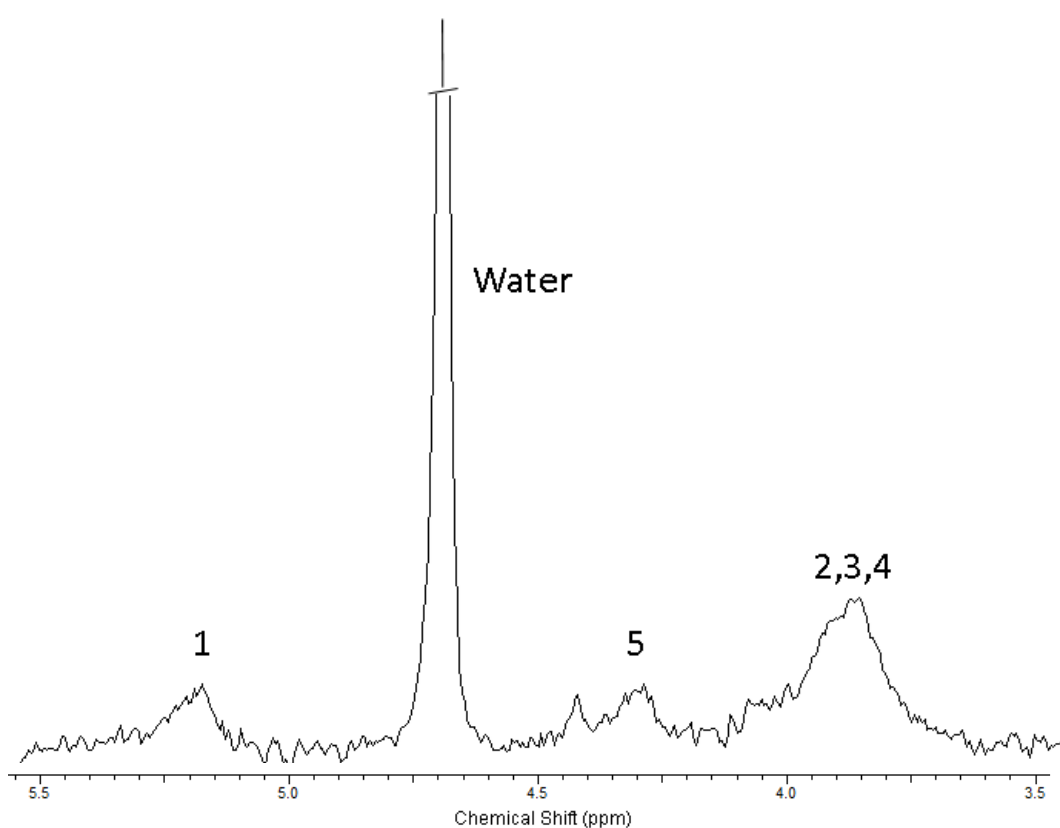


Figure 15- Deuterium spectra of a SPE column purified human urine sample after acetaminophen and deuterated water administration.

Figure 16 shows three spectra of three different samples of the elution phase (10% methanol in acidic water) of the purified AG at different conditions: one sample was put at 50 °C for 24 h, one at 65 °C for 24 h, and the last one was maintained at room temperature (25 °C) and added an acid (TFA) in the NMR at the same time as the sample was loaded.

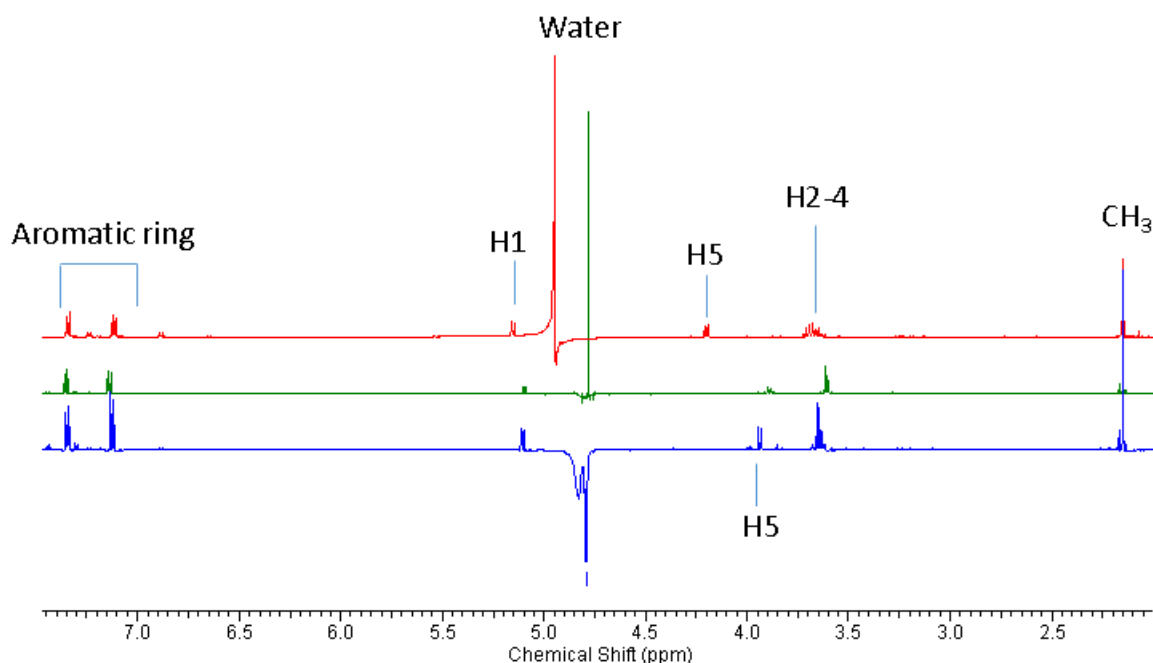


Figure 16-  $^1\text{H}$  NMR spectra of the 10% methanol in acidic water elution phase containing purified urinary AG at different conditions: fraction under 50 °C for 24 h before spectra acquisition (blue), same protocol but at 65 °C (green), adding TFA as the sample is loaded into the NMR tube (red).

Adding TFA to the sample prior to the spectrum acquisition shifted the water signal to higher ppm, but it also shifted the H5 signal in the same direction. Therefore, the resolution of H5 from the water signal was not improved. (Figure 15).

The sample at 50 °C does not show any peak shifts when compared to the sample at room temperature. The  $^1\text{H}$  NMR spectra of the sample under 65 °C shows slight ppm shifts: the methyl group and aromatic ring peaks shift to higher ppm, and the remaining peaks to lower ppm.

A mixture of 10% acetonitrile in distilled water (not showed) was also added to a sample to promote ppm shift. This resulted in a similar effect to increasing the temperature. The water signal shifts to higher fields (lower ppm) and becomes closer to the H5 signal.

The acquisition of  $^{13}\text{C}$  spectra in deuterated water buffered to pH 7.4 with 10 mM sodium phosphate resulted in unexpectedly broad peaks, even though the proton NMR spectra had relatively narrow signals. A second attempt used deuterated water alone to re-suspend the sample and acquire new spectra, but the result was similar to the previous experiment.

Therefore, to obtain better resolved  $^{13}\text{C}$  NMR signals, the AG was hydrolysed into acetaminophen and glucuronic acid. The result from the elution phase with the DSC-18 SPE column was evaporated to dryness. The pellet was re-suspended in 5-8 mL of distilled water and the pH was adjusted to approximately 4.5 by adding a low concentration solution of sodium hydroxide. The acetaminophen-glucuronide was derivatized to glucuronic acid and acetaminophen using 200 units of  $\beta$ -glucuronidase and the solution was incubated at 40 °C for 72 h. The solution was then passed through 1 mL of a cationic resin (Dowex<sup>TM</sup> 50wx8 100-200) [20]. The purified solution was

collected and evaporated to reduce the volume, but without reaching complete dryness. This would result in the closure of the glucuronic acid ring and forming the lactone.

The glucuronic acid was analysed via  $^1\text{H}$  and  $^{13}\text{C}$  NMR spectroscopy. The proton NMR spectra showed well resolved and narrow signals. After that, phosphate buffer with pH 7.4 was added to then evaporate the sample to dryness without converting the glucuronic acid into the lactone. This residue was re-suspended with deuterated water and analysed via  $^{13}\text{C}$  NMR spectroscopy. As for AG, the  $^{13}\text{C}$  NMR spectra of the glucuronic acid had relatively broad  $^{13}\text{C}$  NMR signals (1-2 Hz) that hindered the resolution of  $^{13}\text{C}$ -isotopomer signals in the form of  $^{13}\text{C}$ - $^{13}\text{C}$  coupled spin multiplets (data not shown).

These human samples as well as the the mice samples were later derivatized to MAGL. To note that while mice were administrated deuterated water and carbon-13 tracers, humans were administrated deuterated water only (discussed further on in this thesis).

As mentioned previously, human samples were also derivatized to MAGL. This process used 2 g/12 mL DSC-18 SPE column, and the protocol was the same as for mice, but with volumes scaled up to four times.

## Application of the developed protocol in mice under a High Sugar diet

Several mice were studied in order to assess the impact of a high sugar (HS) diet on hepatic glucose metabolism.

The mice were divided in two groups: control and high sugar diet. The diet was maintained for 18 weeks. Before sacrifice, the mice were administrated deuterated water and acetaminophen, and, from the animals under high sugar diet, half were administrated [U-<sup>13</sup>C]glucose and the other half [U-<sup>13</sup>C]fructose. Mice were transferred to a metabolic cage for 3 days of acclimation. On the last dark period of the last day, they were administrated acetaminophen (all of them), carbon-13 tracers respectively and urine was collected. Mice were not handled by the author of this dissertation.

These experiments are ground breaking not only for using mice for studies involving AG, but also for using [U-<sup>13</sup>C]fructose as a metabolic tracer. Table 1 and Table 2 show novel data about the micromoles of urinary AG and AS present in the urine of each animal (determined by <sup>1</sup>H NMR, using a pyrazine standard), as well as urine volumes excreted by mice and weight variation during a period of 4 months (from the start of the high sugar diet until mice sacrifice).

Table 1- Data from lab mice (C57BL/6), weight variation, urine excretion and acetaminophen derivatives quantification. Mice were under different feeding conditions: normal chow and drinking water (control), high sugar diet (55% fructose and 45% glucose), with [U-<sup>13</sup>C]glucose (HS1) and [U-<sup>13</sup>C]fructose (HS2).

ID	Δ Mice weight (g)	Urine excreted (g)	Body water <sup>2</sup> H enrichment (%)	AG (μmol)	AS (μmol)
CTR A1+A2	4.1	2.16	5.41	35.26	10.23
CTR A3	4.7	2.00	4.19	32.20	9.42
HS1 A1	14.9	4.46	6.58	16.26	3.11
HS1 A2	15.4	3.86	6.65	21.03	3.47
HS2 A1	17.2	2.66	7.27	15.53	4.10
HS2 A2	11.4	2.66	6.18	8.56	1.92
CTR B1	10.2	2.16	5.30	17.83	10.06
CTR B3	8.9	2.00	4.42	28.18	13.81
HS1 B1	13.1	4.46	5.49	48.15	17.71
HS1 B2	14.9	3.86	6.35	54.72	16.26
HS2 B1	10.6	2.66	5.44	15.53	4,10
HS2 B2	11.5	2.66	5.43	22.71	8,02
CTR C1+C2	9.4	5.26	4.86	34.53	15.76
CTR C3	11.5	1.36	4.43	16.14	6.26
HS1 C1	12.2	3.36	6.55	20.67	-
HS1 C2	4.0	3.26	5.77	17.73	-
HS2 C1	8.3	4.56	5.60	19.63	1.97
HS2 C2	11.2	2.06	6.62	14.17	1.74



Table 2- Data from lab mice (C57BL/6), weight variation, urine excretion and acetaminophen derivatives quantification. Aggregation of specimens showed on Table 1 according to the feeding: control and high sugar diet. Average data and standard deviation.

ID	Number of subjects	Δ Mice weight (g)	Urine excreted (g)	BW <sup>2</sup> H enrichment (%)	AG (μmol)	AS (μmol)	AG/AS ratio
Control	6	8.40 ± 0.28*	2.49 ± 0.92	4.77 ± 0.42*	27.36 ± 9.90	10.92 ± 3.14	2.50*
HS	12	11.63 ± 1.94*	3.38 ± 0.72	6.16 ± 0.51*	22.89 ± 9.51	6.24 ± 4.65 <sup>a)</sup>	3.67 <sup>a)</sup> *

<sup>a)</sup> Animals HS1\_C1 and HS1\_C2 show no traces of AS, therefore being excluded of this calculations

\*statistical t-test, comparing differences between control and HS with p<0.05 shows a statistically significant difference between the mentioned groups

This study accounted for a total of three batches of mice, with each batch having three individuals for control, two for HS1 and two for HS2. The values showed above are relative to nine mice (control), and twelve for the High Sugar diet (six for HS1 and six for HS2). The deuterium enrichment quantification of the body water was made in duplicate for each sample.

The urinary yield for AG is, on average, twice-fold as the expected, with high variability between individuals as expected, similarly to human studies [48]. The average AG and AS for each group (A, B and C) are showed in Figure 17, but separated according to the mice feeding (control and high sugar diet). The disparity of results between groups of mice result in high values of standard deviation observed in Table 2.

In this animal groups it was observed that acetaminophen was excreted mostly as AG, as expected from the literature [25,41].

Table 2 shows an increase of the AG/AS ratio when comparing the control and High Sugar mice groups (t-test with p<0.05), with a higher ratio for the HS mice.. The difference between AG and AS for both control and HS groups (separately) is also statistically significant (p<0.05).

These data suggest that the glucuronidation process is more active in mice under high sugar diet in comparison to the conjugation by sulfotransferases. Sulfotransferases availability is dependent of essential amino acids such as methionine and cysteine [49]. Mice that are provided with sugar in their drinking water tend to get fewer calories and nutrients from the solid chow therefore it could be possible that their reduced intake of essential amino acids could be limiting the production of AS in this setting.

Data also suggests that the body water deuterium enrichment achieved was higher, on average, in mice under high sugar diet (t-test with p<0.05). These animals had a higher increase of body weight than control mice because of the dietary intake, having less body water than leaner mice. Control mice increased 1.3 times their initial weight, while mice under high sugar diet increased 1.5 times their initial weight. The administrated deuterated water was more diluted in less heavy mice (control) resulting in less deuterium enrichment overall, while for heavier mice (HS1&2) the body water enrichment was higher. Another interesting set of data shown is the volume of urine excreted by these mice. Although the differences between control and HS groups is not statistically

significant, it is an important set of data to take in count. In the existing literature there is a lack of information relative to this topic.

This thesis presents novel data in this subject, with mice excreting volumes of urine averaging  $2.49 \pm 0.92$  mL and  $3.38 \pm 0.72$  mL, for control and HS groups respectively.

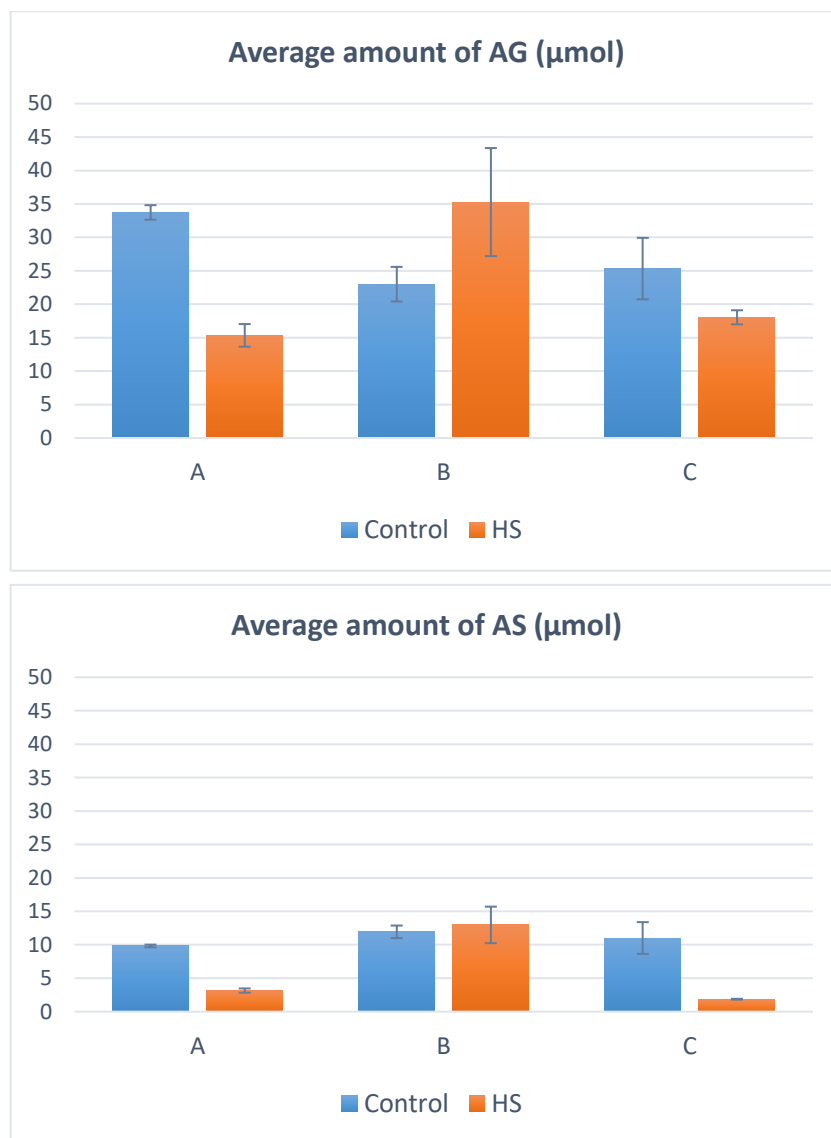


Figure 17- Comparison of the values for the average for mice under control and high sugar diet, separated according to the batch (A, B and C) with standard deviation error bars.

The urine collected was processed using DSC-18 SPE columns, in order to obtain purified AG. Since the AG yields were  $27.36 \pm 9.90$  µmol for control and  $22.89 \pm 9.51$  µmol for animals under high sugar diet, the developed protocol was adapted to columns with a higher capacity than those originally tested. 2 g/12 mL DSC-18 SPE columns were prepared accordingly. The elution phase (10% methanol) was collected and evaporated to dryness. The residue was re-suspended with the appropriate solvents for  $^{13}\text{C}$  and  $^1\text{H}$  NMR (mentioned previously), and spectra were acquired.

## <sup>13</sup>C NMR analysis on mice urine samples after [U-<sup>13</sup>C]fructose and [U-<sup>13</sup>C]glucose administration

AG samples labelled with carbon-13 showed small amounts of enrichment via <sup>13</sup>C NMR spectroscopy and broad peaks, while having <sup>1</sup>H NMR spectra with well-defined and well-resolved peaks.

In order to obtain some results about the carbon-13 enrichment and later compare with the results of other studies being made in parallel, it was performed a derivatization of AG to MAGL. Since previous attempts to hydrolyse AG into glucuronic acid showed no improvements in the <sup>13</sup>C spectra quality, the samples were promptly derivatized to MAGL, since this molecule has narrower <sup>13</sup>C signals. The derivatization protocol followed was the same as described in “Methods” for mice samples.

Figure 18 shows the carbon-13 spectra of a mouse urinary sample where AG was derivatized to MAGL. This mouse was under a high sugar diet and was administrated acetaminophen and [U-<sup>13</sup>C]fructose (HS2). Although <sup>13</sup>C NMR spectra of AG did not show multiplets, suggesting that there was no carbon-13 labelling present, Figure 18 presents evidence that there is carbon labelling and the problem was due to AG carbon-13 spectra’s broad signals (1-2 Hz).

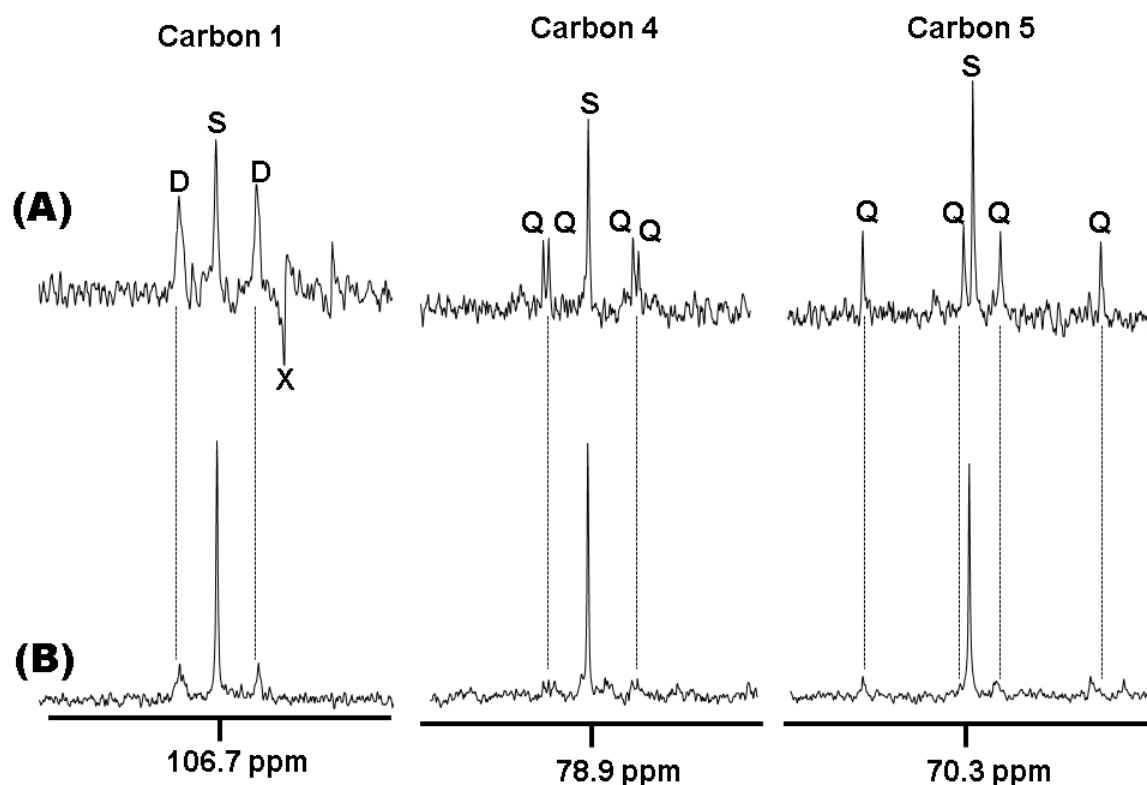


Figure 18- <sup>13</sup>C NMR spectra of MAGL derivatized from urinary AG from mice under high sugar diet (55% fructose and 45% glucose) after administration of acetaminophen. Signals of carbons 1, 4 and 5 are showed, with identification of

singlets (S), doublets (D) and quartets (Q). Mice chow was enriched with 20% [U-<sup>13</sup>C]fructose (HS2) and 20% [U-<sup>13</sup>C]glucose (HS1), correspondent to mouse A and B, respectively.

Most of the mice samples yielded spectra with very low <sup>13</sup>C signal-to-noise ratios, reflecting the limited yield of AG from a single mouse urine collection combined with unavoidable loss of material during the MAGL derivatization process. Finally, samples that yielded spectra with low <sup>13</sup>C signal-to-noise ratios were subject to interference from artifact signals that were clustered in the 80-110 ppm region of the <sup>13</sup>C spectrum, mainly affecting the carbon 1-3 signals.

Figure 18 shows multiplets from the best example spectra obtained from mice provided with [U-<sup>13</sup>C]fructose (A) and [U-<sup>13</sup>C]glucose (B), respectively. The MAGL yield from mouse A was poor, as seen by the low signal-to-noise ratio of the natural abundance singlets (approximately 10:1 signal-to-noise ratio for the singlets) while enrichment from [U-<sup>13</sup>C]fructose was relatively high as seen by the intensities of the <sup>13</sup>C-<sup>13</sup>C coupled multiplet signals relative to the singlet. Since only one spectrum per group was obtained, it is impossible to know if each spectrum is representative of its group. In other words, it is not possible to conclude if the mice that were given [U-<sup>13</sup>C]fructose really had higher glucuronide <sup>13</sup>C-enrichments compared to the mice provided with [U-<sup>13</sup>C]glucose. Qualitatively, the spectra do have <sup>13</sup>C-<sup>13</sup>C multiplet structures that are consistent with previous assignments (Jones et al. [20]). For carbon 1, the doublet (D) signals originate from 1-bond <sup>13</sup>C-<sup>13</sup>C coupling between carbons 1 and 2 ( $J_{C1-C2} = 33.7$  Hz). Long range <sup>13</sup>C-<sup>13</sup>C coupling interactions between carbon 1 and both carbons 3 and 6 cause additional splitting [20] which could not be resolved in these samples. In the spectrum from the mouse fed with [U-<sup>13</sup>C]fructose, the quartet (Q) signals from carbon 4 originate from 1-bond <sup>13</sup>C-<sup>13</sup>C coupling between carbons 4 and 5 ( $J_{C4-C5} = 41.5$  Hz) and 2-bond <sup>13</sup>C-<sup>13</sup>C coupling between carbons 4 and 6 ( $J_{C4-C6} = 1.9$  Hz). The Q signals from carbon 5 originate from 1-bond <sup>13</sup>C-<sup>13</sup>C coupling between carbons 4 and 5 ( $J_{C4-C5} = 41.5$  Hz) and 1-bond <sup>13</sup>C-<sup>13</sup>C coupling between carbons 5 and 6 ( $J_{C5-C6} = 56.5$  Hz). Both sets of Q signals report the same [4,5,6-<sup>13</sup>C<sub>3</sub>]glucuronide isotopomer, which originates from the metabolism of [U-<sup>13</sup>C]fructose to [U-<sup>13</sup>C]triose phosphates followed by indirect pathway incorporation into the triose moieties of glucose-6-phosphate and UDPG.

The hypothesis to justify the lack of carbon-13 labelling is that the mice metabolism is faster than expected. Acetaminophen was administrated before the carbon-13 tracer (glucose and fructose, respectively), and it is possible that it could have been metabolized to AG ahead of the <sup>13</sup>C-enriched sugars.

Since some peaks of the MAGL spectra acquired show traces of carbon-13 labelling, even if they have low signal-to-noise ratio doublets, it is safe to assume that the acetaminophen and the <sup>13</sup>C tracers did not “miss each other” completely in the hepatic glycogenesis. This hypothesis is furthermore supported by the fact that a parallel experiment (performed by other scientists) involving glycogen isolation and purification from the livers of these mice, followed by its derivatization to MAG, showed high intensity multiplets, with high signal-to-noise ratios.

## $^2\text{H}$ NMR analysis of mice urinary samples with deuterium labelling from deuterated water

While  $^{13}\text{C}$ -enrichment of AG from the dietary sugars is dependent on the mice ingesting the sugar followed by conversion to UDPG, AG enrichment from  $^2\text{H}$  might have occurred sooner because this  $^2\text{H}_2\text{O}$  was injected in a single dose at the same time that acetaminophen was administered.  $^2\text{H}_2\text{O}$  equilibrates very rapidly with body water and would have been present in the liver within minutes of being administered.

As showed previously in Figure 15,  $^2\text{H}$  spectra of AG presented broad signals. It is expected that, since the samples underwent derivatization to MAGL, the signals are narrower and have a higher signal-to-noise ratio.  $^2\text{H}$  spectra acquired from mice samples are only of MAGL.

Figure 19 shows a spectrum of MAGL obtained from the derivatization of urinary AG. The sample is from mice that were under a high sugar diet (55% fructose and 45% glucose). This spectrum has signals that are considerably narrower than those of native AG showed in Figure 15. The referenced signals are from the glucuronide moiety. Signal 1 width is 1.2 Hz, signal 4 is 1.44 Hz, signals 2 and 3 are 2.9 Hz, signal 5 is 2.14 Hz..

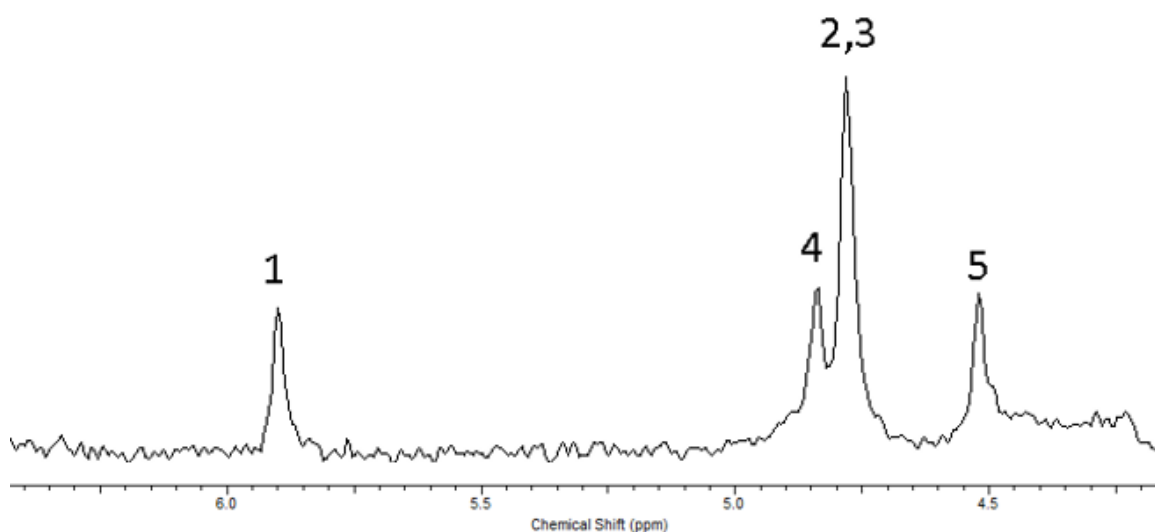


Figure 19 –  $^2\text{H}$  spectrum of MAGL derivatized from urinary AG of a single mouse fed on the high sugar diet and administrated with deuterated water. Signals 1-5 are identified in the spectrum.

Similarly to the results showed and described for  $^{13}\text{C}$  NMR, since there are only spectra from mice that were under high sugar diet and no control spectra were acquired, it is impossible to know if this  $^2\text{H}$  spectrum is representative of its group.

The methyl groups from the deuterated acetone were incorporated into the derivatization end product (MAGL). The methyl signals appear at 1.32 ppm and 1.49 ppm (not shown). By knowing the deuterium enrichment of these signals (2.26%), they can work as an internal reference, making

it is possible to calculate the relative intensity of each signal from the glucuronide moiety of MAGL. Taking in consideration the deuterium labelling of the acetone used (2.26%), it is feasible to calculate the absolute deuterium enrichment for the isolated signals:  $^2\text{H}1 = 1.47\%$  and  $^2\text{H}5 = 1.42\%$ . Since signals 2 and 3 are overlapped, they cannot be individually quantified, but the sum of  $^2\text{H}2$  and  $^2\text{H}3$  signals show 5.26% of deuterium enrichment.  $^2\text{H}4$  is partially overlapped by the signals 2 and 3, making it impossible to quantify with certainty, but approximately  $^2\text{H}4 = 1.99\%$ .

This specific mouse is denominated as HS2 C2 and has a body water deuterium enrichment of 6.62% (Table 1). The relative contributions of the direct and indirect pathways are estimated to be 21.38% and 78.62%, respectively.

Compared with previous assignments [18, 32, 35], the values for the deuterium enrichment for all positions are higher. This difference could be due to the fact that this dissertation uses mice as animal models, while the mentioned articles report experiments done in human subjects. Moreover, the mice weight increase, lowers the amount of body water. This increases the overall concentration of deuterium after the IP injection of deuterated water, explaining the high body water deuterium enrichment and the MAGL  $^2\text{H}$  enrichment.

The indirect pathway shows a lower percentage when compared with previous studies (Jarak, et al. 2019 [35]). Glucose is being the major contributor to the hepatic glycogenesis and this could be explained by the fructose being used in other metabolic pathways and/or that the fructose is stimulating a glycolytic enzyme, such as glucokinase, that would increase the direct pathway relative contribution.

A parallel study being performed using the mice mentioned in this dissertation, in which the hepatic glycogen was isolated, purified, broken into hexose units and derivatized into MAG, showed similar indirect pathway relative contribution (20%). This study presented body water deuterium enrichment of 6.18%. The fact that both this values are in accordance to the ones showed in this dissertation suggests that the  $^2\text{H}$  spectrum in Figure 19 is representative.

Assuming that most MAGL was labelled with deuterium from the deuterated water administrated, the low signal-to-noise signals observed in Figure 19 is caused by the derivatization protocol losing a lot of material or not sufficient amount of the starting material (AG) to begin with. Knowing the results yielded by  $^{13}\text{C}$  NMR spectroscopy, the most likely scenario is that mice are not excreting sufficient glucuronide to acquire spectra with a high signal-to-noise ratio. Proceeding to the derivatization to MAGL provided spectra with better quality signals, but did not compensate for the low amount of material.

# Conclusion

---

The newly developed protocol for AG purification from urine samples that uses DSC18 SPE-columns showed great results, providing yields averaging  $85.2\% \pm 4.5\%$  of purified AG. The protocol is based on the one described by Burgess et al. [19]. This protocol was adapted to mice, since this dissertation was focused on animal studies, and was optimized for greater yields.

The 1 g/6 mL DSC18 SPE-column preparation consists in 6 mL of 100% methanol followed by 20 mL of acidic water (0,024% TFA). The sample pH is lowered to 2-2.5 pH using TFA and then loaded into the column. If the sample contains more or less than 10  $\mu\text{mol}$  in 1 mL of sample, either evaporate some of the water in the sample/dilute the sample with distilled water respectively, or use a higher/lower capacity column for the desired sample. After loading the sample into the column, wash with 5mL of acidic water (0,024% TFA) and elute with 10% methanol in acidic water. The elution phase will contain the purified AG. A final wash using 100% methanol can be performed if desired.

The AG showed stability for long periods of time (more than six months) at room temperature, and at 50 °C and 65 °C for 24 h. The stability tests at high temperature were performed in a purified fraction of AG corresponding to the 10% MeOH elution phase. This molecule does not show any particular signs of bacterial degradation or contamination when present in urine.

This study showed different values of AG and AS in mice urine, changing between the control group and animals under high sugar diet. The control group presented an average of  $27.36 \pm 9.90$   $\mu\text{mol}$  of AG and  $10.92 \pm 3.14$   $\mu\text{mol}$  of AS in  $2.49 \pm 0.92$  mL of urine excreted. Mice under high sugar diet were separated into two groups only differentiated by the  $^{13}\text{C}$  labelling administered the day prior to the sacrifice, meaning that both had the same diet. The overall high sugar group (HS1 and HS2) showed  $22.89 \pm 9.51$   $\mu\text{mol}$  of AG and  $6.24 \pm 4.65$   $\mu\text{mol}$  of AS excreted in  $3.38 \pm 0.72$  mL of urine

To note that the body water deuterium enrichment also presented in this thesis had higher values for the group under high sugar diet, than those from the control group. The high sugar diet induces weight gain, lowering the total body water amount in those animals, therefore lowering the overall body water deuterium enrichment.

AG proton NMR showed well-resolved and defined peaks, with signals H1 and H5 isolated. The present study had primary focus on the signal 5, because it gives information about the glucose metabolism pathway activity: when administrated deuterated water, the position 5 is labelled in the indirect pathway, but not in the direct pathway, providing a way to distinguish between both.

AG carbon-13 NMR spectra did not show multiplets because the peaks were too broad (1-2 Hz). Derivatization protocol of AG to MAGL followed.  $^{13}\text{C}$  NMR spectra were acquired and showed multiplets with a low signal-to-noise ratio. Spectra of samples from mice administered tracer  $[\text{U-}^{13}\text{C}]\text{glucose}$  had a lower enrichment than those that were administered  $[\text{U-}^{13}\text{C}]\text{fructose}$ . Since only one spectrum per group was obtained, it is impossible to know if each spectrum is representative of its group.

From a qualitative point of view, the carbon-13 spectra show  $^{13}\text{C}$ - $^{13}\text{C}$  multiplets that are consistent with data present in previous studies [20].

This results are an indication that the mice metabolism is faster than expected. The administered acetaminophen was metabolized before the carbon-13 labelled tracer reached the liver, providing little labelling to the urinary AG.

AG  $^2\text{H}$  NMR spectra had broad peaks (3-8 Hz). MAGL deuterium spectra obtained from the derivatization mentioned above had narrower signals (1-3 Hz). Similarly to the carbon-13 results, the single spectrum showed could not be representative of the whole high sugar diet group.

The mouse was administered deuterated water (99,9%) via IP injection in order to achieve 4% deuterium body water enrichment but presented a body water enrichment of 6.62% due to the weight gain, as explained previously.  $^2\text{H}$  MAGL spectrum acquired from a urine sample from a mouse that was under a high sugar diet showed a relative contribution of 21.38% to the indirect pathway, being consistent with results from a parallel experiment using MAG derivatized from hepatic glycogen from the same animal model. This presents solid evidence that the results are accurate.

The  $^2\text{H}$  NMR results for AG and MAGL furthermore support the hypothesis that was mentioned for the  $^{13}\text{C}$  NMR results: the starting amount of material was not enough to proceed to NMR experiments, making it impossible to make a quantitative study and assess about the hepatic glycogenesis and the fate of the administered carbon-13 tracers, specifically  $[\text{U-}^{13}\text{C}]\text{glucose}$  and  $[\text{U-}^{13}\text{C}]\text{fructose}$ .



# Future Perspectives

---

In future experiments it would be in the best interest to remake the mice experiments in the same conditions and same high sugar diet. Using 3 groups: controls fed standard chow only, standard chow diet plus high sugar diet enriched [U-<sup>13</sup>C]glucose in the drinking water and another group under high sugar diet enriched with [U-<sup>13</sup>C]fructose, but with some modifications. The carbon-13 results in this thesis were compromised because of the acetaminophen administration (10 mg of acetaminophen/100 g of body weight). To solve this, it is proposed a protocol with a lower dosage of acetaminophen (5 mg/100 g) administered twice during the last dark cycle: two times in periods of 6 h, instead of a single administration for 12 h. This change would ensure a greater incorporation of [U-<sup>13</sup>C] tracers in the acetaminophen-glucuronide, increasing the signal-to-noise ratio of the <sup>13</sup>C NMR spectra and allow further assessments to be made about the pathways that each tracer took. Another approach that could grant a more reliable NMR spectra and data is to increase the amount of material per sample. Since the described methods are non-invasive, this study could be performed several times in the same mouse (2-3 times). Pooling the urine samples of each mouse would increase the amount of glucuronide by 2-3 times. Note that this protocol demands an interval of 2-3 weeks in between each tracer administration to allow the previous tracers to fully wash out. This approach could also be used to improve deuterium NMR results, increasing the signal-to-noise ratio of the spectra. Following this protocol could ensure better <sup>2</sup>H NMR spectra, allowing for the signals to be quantified and make assessments about the direct and indirect pathways, specifically their relative contributions to glycogenesis.

The non-invasive character of this protocol would also allow a subject selection based on urinary AG yields. Mice would be administered acetaminophen, without tracers, to assess urinary AG yields. This would allow the selection of mice with higher AG yields for the labelling study. The risk of this approach is that it might be inadvertently selecting a particular metabolic phenotype (high glucuronide producer) that would not be representative of the general mice population. Also, mice that are genetically modified and/or diseased may also have different rates of glucuronide production than wild-type healthy animals. To account for this variable, these healthy animals would need to be tested beforehand.

It would also be interesting to acquire a significant number of <sup>2</sup>H and <sup>13</sup>C NMR spectra and combine results in order to comprehend in a more complete way the action of the metabolic pathways in mice under high sugar diet, and what differs for glucose and fructose in those pathways.

# References

---

- [1] N. H. Cho *et al.*, “IDF Diabetes Atlas: Global estimates of diabetes prevalence for 2017 and projections for 2045,” *Diabetes Res. Clin. Pract.*, vol. 138, pp. 271–281, 2018.
- [2] A. Fuller and C. Stegeman, “Type 1 and Type 2 Diabetes,” *Pediatr. Adult Nutr. Chronic Dis. Dev. Disabil. Hered. Metab. Disord.*, vol. 12, no. 2, pp. 334–336, 2017.
- [3] D. Control and P. Cdc, “National Diabetes Statistics Report , 2017 Estimates of Diabetes and Its Burden in the United States,” 2017.
- [4] C. L. *et al.*, “Origins and evolution of the Western diet: Health implications for the 21st century,” *Am. J. Clin. Nutr.*, vol. 81, no. 2, pp. 341–354, 2005.
- [5] K. Parker, M. Salas, and V. C. Nwosu, “High fructose corn syrup: Production, uses and public health concerns,” *Biotechnol. Mol. Biol. Rev.*, vol. 5, no. 5, pp. 71–78, 2010.
- [6] M. I. Goran, S. J. Ulijaszek, and E. E. Ventura, “High fructose corn syrup and diabetes prevalence: A global perspective,” *Glob. Public Health*, vol. 8, no. 1, pp. 55–64, 2013.
- [7] G. A. Bray, S. J. Nielsen, and B. M. Popkin, “Consumption of high-fructose corn syrup in beverages may play a role in the epidemic of obesity,” *Am. J. Clin. Nutr.*, vol. 79, no. 4, pp. 537–543, 2004.
- [8] B. C. P. F. F. Toldra, *Encyclopedia of Food Sciences and Nutrition*, 2nd ed. 2003.
- [9] E. Pamies-Andreu, M. Fiksen-Olsen, R. A. Rizza, and J. C. Romero, “High-fructose feeding elicits insulin resistance without hypertension in normal mongrel dogs,” *Am. J. Hypertens.*, vol. 8, no. 7, pp. 732–738, 1995.
- [10] F. Akar *et al.*, “High-fructose corn syrup causes vascular dysfunction associated with metabolic disturbance in rats: Protective effect of resveratrol,” *Food Chem. Toxicol.*, vol. 50, no. 6, pp. 2135–2141, 2012.
- [11] I. Zavaroni, S. Sander, S. Scott, and G. M. Reaven, “Effect of fructose feeding on insulin secretion and insulin action in the rat,” *Metabolism.*, vol. 29, no. 10, pp. 970–973, 1980.
- [12] E. Campbell, A. Schlappal, E. Geller, and T. Castonguay, “Fructose-Induced Hypertriglyceridemia: A Review,” *Nutr. Prev. Treat. Abdom. Obes.*, pp. 197–205, Mar. 2014.
- [13] L. Tappy, K. A. Lê, C. Tran, and N. Paquot, “Fructose and metabolic diseases: New findings, new questions,” *Nutrition*, vol. 26, no. 11–12, pp. 1044–1049, 2010.
- [14] A. Lindqvist, A. Baelemans, and C. Erlanson-Albertsson, “Effects of sucrose, glucose and fructose on peripheral and central appetite signals,” *Regul. Pept.*, vol. 150, no. 1–3, pp. 26–32, 2008.
- [15] J. J. López-Soldado, I. Zafra, D., Duran, J., Adrover, A., Calbó, J., & Guinovart, “Liver glycogen reduces food intake and attenuates obesity in a high-fat diet-fed mouse model,” *Diabetes*, vol. 64(3), no. 615, pp. 796–807, 2014.
- [16] J. E. Pessin and A. R. Saltiel, “Signaling pathways in insulin action: Molecular targets of insulin resistance,” *J. Clin. Invest.*, vol. 106, no. 2, pp. 165–169, 2000.
- [17] A. Ribeiro *et al.*, “Simple measurement of gluconeogenesis by direct<sup>2</sup>H NMR analysis of menthol glucuronide enrichment from<sup>2</sup>H<sub>2</sub>O,” *Magn. Reson. Med.*, vol. 54, no. 2, pp. 429–434, 2005.
- [18] C. Barosa, J. G. Jones, R. Rizza, A. Basu, and R. Basu, “Acetaminophen glucuronide and plasma glucose report identical estimates of gluconeogenesis and glycogenolysis for healthy and prediabetic subjects using the deuterated water method,” *Magn. Reson. Med.*, vol. 70, no. 2, pp. 315–319, 2013.
- [19] S. C. Burgess *et al.*, “Noninvasive evaluation of liver metabolism by <sup>2</sup>H and <sup>13</sup>C NMR isotopomer analysis of human urine,” *Anal. Biochem.*, vol. 312, no. 2, pp. 228–234, 2003.
- [20] J. Jones *et al.*, “NMR Derivatives for quantification of <sup>2</sup>H and <sup>13</sup>C-enrichment of human glucuronide from metabolic tracers,” *J. Carbohydr. Chem.*, vol. 25, no. 2–3, pp. 203–217, 2006.
- [21] Y. Cho, Y. Jang, Y. D. Yang, C. H. Lee, Y. Lee, and U. Oh, “TRPM8 mediates cold and

- menthol allergies associated with mast cell activation,” *Cell Calcium*, vol. 48, no. 4, pp. 202–208, 2010.
- [22] E. Bakkeheim, P. Mowinckel, K. H. Carlsen, G. Håland, and K. C. L. Carlsen, “Paracetamol in early infancy: The risk of childhood allergy and asthma,” *Acta Paediatr. Int. J. Paediatr.*, vol. 100, no. 1, pp. 90–96, 2011.
- [23] J. A. H. Forrest, J. A. Clements, and L. F. Prescott, “Clinical Pharmacokinetics of Paracetamol,” *Clin. Pharmacokinet.*, vol. 7, no. 2, pp. 93–107, 1982.
- [24] M. K. Hellerstein, D. J. Greenblatt, and H. N. Munro, “Glycoconjugates as noninvasive probes of intrahepatic metabolism: I. Kinetics of label incorporation with evidence of a common precursor UDP-glucose pool for secreted glycoconjugates,” *Metabolism*, vol. 36, no. 10, pp. 988–994, 1987.
- [25] IARC, “Paracetamol (Acetaminophen) Chemical and physical data,” *Pharm. Drugs IARC Monogr. Eval. Carcinog. Risks to Humans*, no. 50, p. 415, 1990.
- [26] Cayman Chemical, “Bafilomycin A1 Section 1 . Identification of the Substance / Mixture and of the Company / Undertaking Section 2 . Hazards Identification Bafilomycin A1 Section 4 . First Aid Measures Section 5 . Fire Fighting Measures,” vol. 47700, no. 1907, 2016.
- [27] L. James, J. E. Sullivan, and D. Roberts, “The proper use of acetaminophen,” *Paediatr. Child Health (Oxford)*, vol. 16, no. 9, pp. 544–547, 2011.
- [28] D. Administration *et al.*, “Benefit risk profile of Acetylcysteine in the management of paracetamol overdose,” *Crit. Care Secrets Fourth Ed.*, vol. 16, no. June, pp. 1–4, 2012.
- [29] G. B. Steventon, S. C. Mitchell, and R. H. Waring, “Human metabolism of paracetamol (acetaminophen) at different dose levels.,” *Drug Metabol. Drug Interact.*, vol. 13, no. 2, pp. 111–7, 1996.
- [30] J. Miners, J. F. Adams, and D. J. Birkett, “a Simple Hplc Assay for Urinary Paracetamol Metabolites and Its Use To Characterize the C3H Mouse As a Model for Paracetamol Metabolism Studies,” *Clin. Exp. Pharmacol. Physiol.*, vol. 11, no. 2, pp. 209–217, 1984.
- [31] A. F. Soares, R. A. Carvalho, F. J. Veiga, and J. G. Jones, “Effects of galactose on direct and indirect pathway estimates of hepatic glycogen synthesis,” *Metab. Eng.*, vol. 12, no. 6, pp. 552–560, 2010.
- [32] J. G. Jones *et al.*, “Noninvasive analysis of hepatic glycogen kinetics before and after breakfast with deuterated water and acetaminophen,” *Diabetes*, vol. 55, no. 8, pp. 2294–2300, 2006.
- [33] T. C. Delgado *et al.*, “<sup>2</sup>H enrichment distribution of hepatic glycogen from <sup>2</sup>H<sub>2</sub>O reveals the contribution of dietary fructose to glycogen synthesis.,” *Am. J. Physiol. Endocrinol. Metab.*, vol. 304, no. 4, pp. E384-91, 2013.
- [34] F. Diraison, C. Pachaiaudi, and M. Beylot, “In vivo measurement of plasma cholesterol and fatty acid synthesis with deuterated water: Determination of the average number of deuterium atoms incorporated,” *Metabolism*, vol. 45, no. 7, pp. 817–821, 1996.
- [35] I. Jarak *et al.*, “Sources of hepatic glycogen synthesis in mice fed with glucose or fructose as the sole dietary carbohydrate,” *Magn. Reson. Med.*, vol. 81, no. 1, pp. 639–644, 2019.
- [36] I. Y. Choi, I. Tkáč, K. Uğurbil, and R. Gruetter, “Noninvasive measurements of [1-<sup>13</sup>C]glycogen concentrations and metabolism in rat brain in vivo,” *J. Neurochem.*, vol. 73, no. 3, pp. 1300–1308, 1999.
- [37] C. Wehmeyer, N., Gunderson, H., Nauman, J., Savage, S., & Hartzell, “Determination of the glycogen synthesis pathway by <sup>13</sup>C nuclear magnetic resonance analysis,” *Metabolism*, vol. 43, pp. 38–43, 1994.
- [38] E. S. Jin, A. D. Sherry, and C. R. Malloy, “Interaction between the pentose phosphate pathway and gluconeogenesis from glycerol in the liver,” *J. Biol. Chem.*, vol. 289, no. 47, pp. 32593–32603, 2014.
- [39] R. Perdigoto, T. B. Rodrigues, A. L. Furtado, A. Porto, C. F. G. C. Geraldes, and J. G. Jones, “Integration of [U-<sup>13</sup>C]glucose and 2H<sub>2</sub>O for quantification of hepatic glucose production and gluconeogenesis,” *NMR Biomed.*, vol. 16, no. 4, pp. 189–198, 2003.
- [40] J. Jones, S. Kahl, F. Carvalho, C. Barosa, and M. Roden, “Simplified analysis of acetaminophen glucuronide for quantifying gluconeogenesis and glycogenolysis using

- deuterated water,” *Anal. Biochem.*, vol. 479, pp. 37–39, 2015.
- [41] B. S. A. Silva *et al.*, “Resistance exercise training improves mucociliary clearance in subjects with COPD: A randomized clinical trial,” *Pulmonology*, vol. 25, no. 6, pp. 340–347, 2019.
- [42] C. Barosa, M. Almeida, M. M. Caldeira, F. Gomes, and J. G. Jones, “Contribution of proteolytic and metabolic sources to hepatic glutamine by  $^2\text{H}$  NMR analysis of urinary phenylacetylglutamine  $^2\text{H}$ -enrichment from  $^2\text{H}_2\text{O}$ ,” *Metab. Eng.*, vol. 12, no. 1, pp. 53–61, 2010.
- [43] A. F. Soares, F. J. Viegas, R. A. Carvalho, and J. G. Jones, “Quantifying hepatic glycogen synthesis by direct and indirect pathways in rats under normal ad libitum feeding conditions,” *Magn. Reson. Med.*, vol. 61, no. 1, pp. 1–5, 2009.
- [44] S. Cerdan and J. Seelig, “NMR studies of metabolism,” *Annu. Rev. Biophys. Biophys. Chem.*, vol. 19, pp. 43–67, 1990.
- [45] C. DOW, “Dowex-50-WX8-50-100-resin,” *Trademark Dow Chem. Co.*, vol. 117-01509-, p. 9, 1990.
- [46] J. G. Jones, M. Merritt, and C. Malloy, “Quantifying tracer levels of  $^2\text{H}_2\text{O}$  enrichment from microliter amounts of plasma and urine by  $^2\text{H}$  NMR,” *Magn. Reson. Med.*, vol. 45, no. 1, pp. 156–158, 2001.
- [47] P. Types, “Ion exchange packings Normal phase SPE Ion exchange SPE,” 1998.
- [48] J. R. Bales, P. J. Sadler, J. K. Nicholson, and J. A. Timbrell, “Urinary excretion of acetaminophen and its metabolites as studied by proton NMR spectroscopy,” *Clin. Chem.*, vol. 30, no. 10, pp. 1631–1636, 1984.
- [49] W. Boles and C. D. Klaassen, “The importance phosphosulfate ( PAPS ) in the regulation of sulfation,” *FASEB J.*, vol. 11, pp. 404–418, 1997.